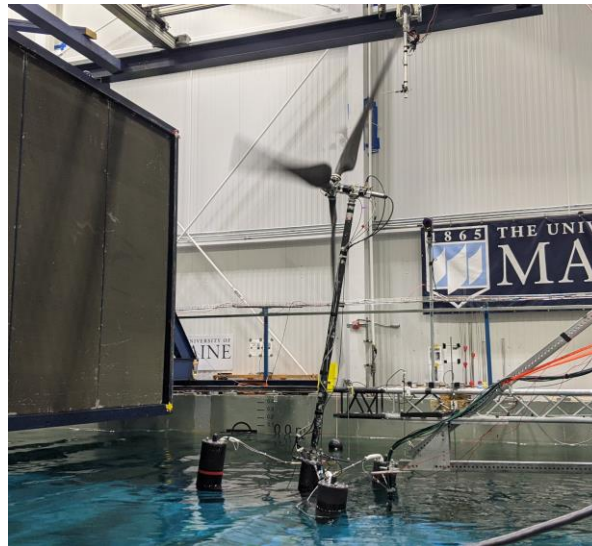


Floating Offshore Wind Controls Advanced Laboratory (FOCAL) Experimental Program – Campaign 4

1:70 Model-Scale Test of the IEA-Wind 15MW Reference Turbine and VoltturnUS-S Platform

Testing Summary and Data Report



Prepared for:

National Renewable Energy Laboratory

University of Maine’s Advanced Structures and Composites Center

Report Number: 23-57-1183

| Author | Reviewer | Date | Version |
|------------------|-------------------------|-----------|---------|
| Eben Lenfest, MS | Matthew Fowler, MS, MBA | 4/27/2023 | - |
| | | | |
| | | | |

This report shall not be reproduced, except in full, without the written approval of University of Maine’s Advanced Structures and Composites Center.



An ISO 17025 accredited testing laboratory, accredited by the International Accreditation Service

The Advanced Structures and Composites Center is an ISO 17025 accredited testing laboratory with over 20 years of testing experience meeting industry standards from coupon-scale to full-scale. This certifies that we have met the requirements of the IAS Accreditation Criteria for Testing Laboratories (AC89), and demonstrated compliance with ISO/IEC Standard 17025, General Requirements for the Competence of Testing and Calibration Laboratories, and are accredited for the test methods listed in the approved scope of accreditation. While the testing described herein does not specifically fall under our ISO 17025 scope of accreditation, the procedures outlined in our quality system applies to all of our laboratory activities (as much as possible) signifying our commitment to a high standard of quality including testing methodology, instrumentation, and reporting. Please contact our facility if further information is required.

Table of Contents

| | |
|--|-----------|
| 1. Introduction..... | 1 |
| 2. Facilities and Conventions | 2 |
| <i>Description of the Harold Alfond W² Ocean Engineering Laboratory</i> | <i>2</i> |
| <i>Orientation and Coordinate Systems</i> | <i>4</i> |
| <i>Wave Measurement Locations</i> | <i>6</i> |
| 3. Scaling Methodology..... | 7 |
| <i>Turbine Scaling Methodology.....</i> | <i>7</i> |
| <i>Wind Speed Adjustments</i> | <i>8</i> |
| <i>Water Density Mismatch.....</i> | <i>8</i> |
| 4. System Properties..... | 10 |
| <i>Hull Properties.....</i> | <i>16</i> |
| <i>Tuned Mass Damper Properties</i> | <i>17</i> |
| <i>Mooring Properties.....</i> | <i>18</i> |
| <i>Tower Properties</i> | <i>20</i> |
| <i>RNA Properties</i> | <i>21</i> |
| 5. Turbine Controller..... | 23 |
| <i>Floating Feedback</i> | <i>24</i> |
| <i>Peak Shaving.....</i> | <i>25</i> |
| 6. Instrumentation and Data Acquisition | 26 |
| <i>A Note on Rotor Thrust.....</i> | <i>27</i> |
| <i>Internal Load Cells</i> | <i>27</i> |
| <i>Data Post-Processing</i> | <i>28</i> |
| 7. Test Program | 29 |
| <i>Wind Conditions.....</i> | <i>29</i> |
| <i>Wave Conditions</i> | <i>31</i> |
| <i>Test Matrices.....</i> | <i>34</i> |
| Bibliography | 38 |
| Appendix A: Model Drawings | 39 |
| Appendix B: Airfoil Properties..... | 46 |
| Appendix C: OpenFAST Model | 50 |

1. Introduction

The Floating Offshore-wind and Controls Advanced Laboratory (FOCAL) Experimental Program will create the first public floating offshore wind turbine (FOWT) 1:70 scale 15-MW model-test dataset to include advanced turbine controls, floating hull load mitigation technology, and hull flexibility. To effectively utilize a control co-design (CCD) approach as envisioned by ARPA-E, coupled aeroelastic-hydrodynamic software must be validated with experimental data. This project aims to generate these data to advance the ARPA-E objectives and enable lower-cost FOWT systems.

The FOCAL program consists of a series of four model-scale FOWT experimental campaigns in UMaine's Alford Wind-Wave Ocean Engineering Laboratory (W2) laboratory (Figure 1).

The four campaigns are:

- Campaign 1) Advanced Wind Turbine Control Strategies,
- Campaign 2) Active Hull Controls,
- Campaign 3) Hull Flexibility, and
- Campaign 4) System-level Control Strategy.

The experiments address two notable limitations of existing experimental datasets. First, prior experimental campaigns utilized completely rigid model-scale platforms, preventing meaningful study of the influence of flexibility on the system response. Second, these experiments only considered limited control strategy implementation – either for the turbine or the platform.

To perform the experimental campaigns, FOCAL uses a performance-matched, scale-model wind turbine based on the newly developed IEA-Wind 15-MW Reference Wind Turbine (Gaertner, Evan et al., 2020). The scale model is capable of simulating advanced blade pitch control strategies in the high-quality wind fields generated in the W2 and is fully instrumented to record a variety of parameters in real time including structural loads and dynamics.

This report documents Campaign 4, where the turbine is mounted to a flexible tower and deployed on the scale floating platform for a fully-coupled wind/wave test campaign. The system is subject to a variety of wind and wave conditions representing operational as well as design driving environments. System dynamics and turbine characteristics are measured to determine global performance and assess the effect of the control strategies employed. NREL's Reference Open-Source Controller (ROSCO) is employed for active blade pitch control, with and without the addition of floating feedback and peak shaving. Hull structural control is also examined using tuned mass dampers (TMDs) tuned to the system's natural pitch and tower bending frequencies.

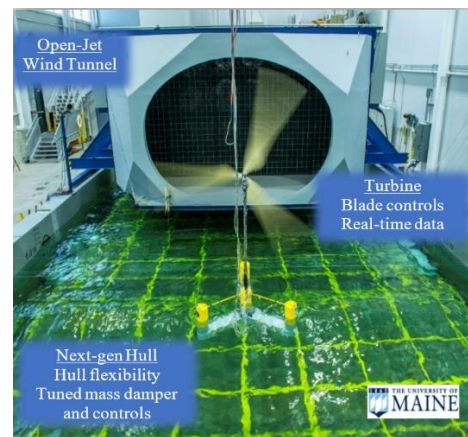


Figure 1. UMaine's Wind/Wave Lab

2. Facilities and Conventions

Description of the Harold Alfond W² Ocean Engineering Laboratory¹

UMaine's Advanced Structures and Composites Center, shown in Figure 2, is an ISO 17025 accredited interdisciplinary research and testing center dedicated to the development of novel advanced composite materials and technologies. The total facility size is over 9,200 m² and was established in 1996 by the National Science Foundation.



Figure 2: Advanced Structures and Composites Center at the University of Maine

Shown in Figure 3, W² is a deep multi-paddle wave basin with an integrated, rotatable wind tunnel which permits simultaneous application of scaled wind and wave environments for sophisticated floating body model tests. The facility can accurately simulate towing tests, variable water depths, and scaled wind and wave conditions for many offshore sites.

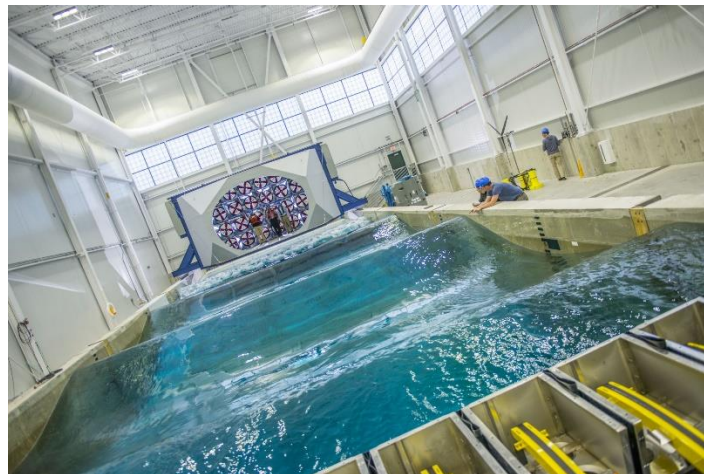


Figure 3: W² wind/wave basin at UMaine

¹ Please note dimensions in this section are provided at actual scale unless otherwise noted.

The basin dimensions, shown in Figure 4, are 30 m long \times 9 m wide with adjustable floor for water depths 0-5.0 m.

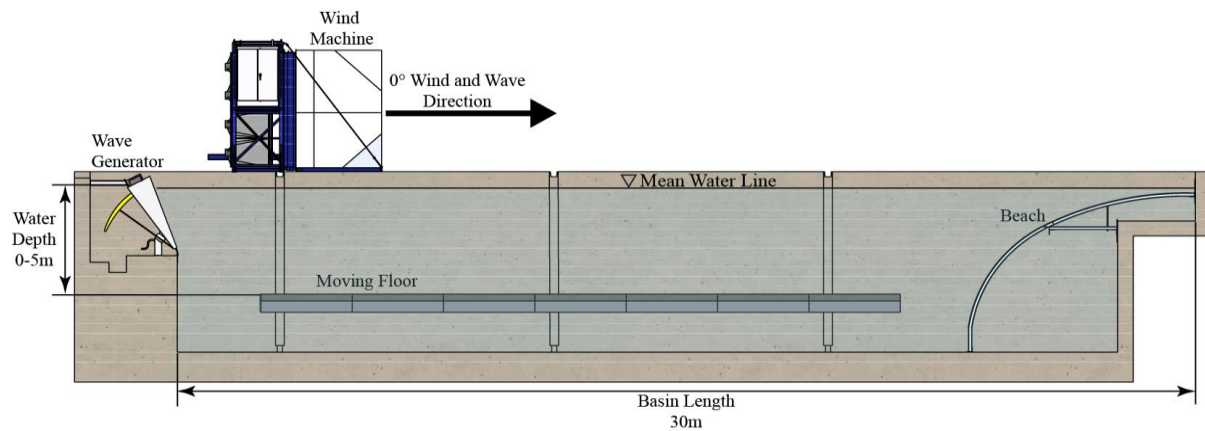


Figure 4: Basin Schematic and Dimensions

Waves were generated using a 16-paddle wave maker capable of simulating regular waves, standard spectra waves, and custom random sea states with directional waves and range frequencies. The wave maker's capabilities include:

- Angles in excess of ± 60 degrees relative to the basin centerline
- Maximum heights of 0.6m at $T=1.65$ seconds, and 0.8m at $T=2.3$ seconds
- Beach: design reflection $\leq 7\%$ for all relevant wave frequencies

Wind is generated using a bank of fans arranged in a 4 row by 8 column grid (Figure 5). The overall properties of the wind system are:

- Test Area Dimensions: 7.0 m \times 3.5 m (width \times height)
- Wind speed: 0 to 12 m/s
- Steady-state, Turbulent, and Non-Uniform (e.g. wind shear) wind fields
- Non-Uniformity: $<10\%$
- Steady-state Turbulence: $<5\%$
- Flow direction relative to waves: 0 to 180 degrees. Movable with overhead crane.

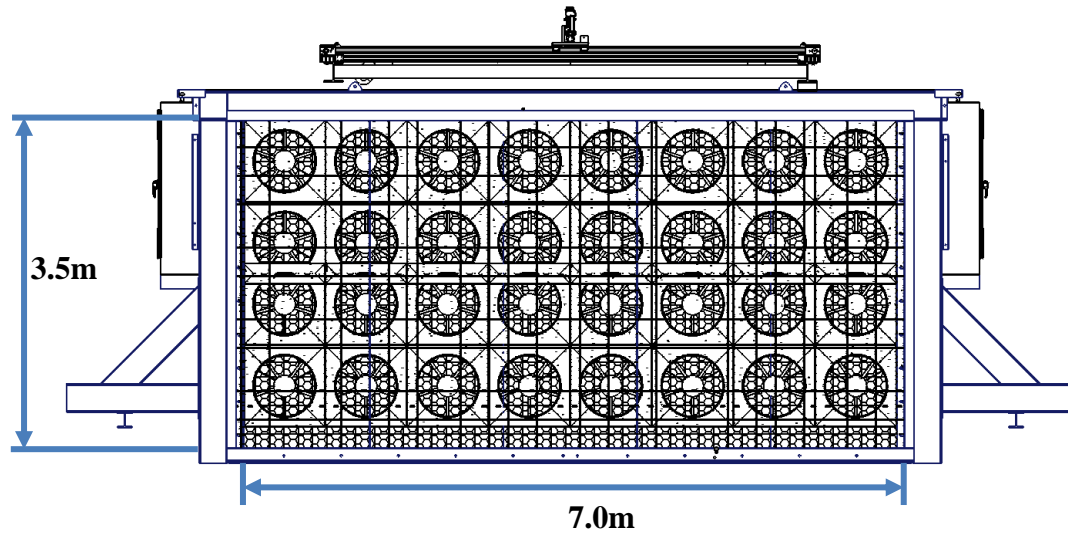


Figure 5: Wind Machine Elevation View

Orientation and Coordinate Systems

The general basin layout is shown in Figure 6. This global coordinate system is used to report, for example, the location of the turbine model or wind generator in the wave basin. Figure 6 also indicates the nominal location of the floating platform for Campaign 4. The relevant notations in terms of platform local coordinates and motion definitions are provided in Figure 7. Turbine load time-history measurements recordings will be taken in the local coordinate system (unless otherwise noted), where the origin is as shown in Figure 7. Mooring tensions are reported in the local fairlead coordinate systems, with tension in the line being presented as positive as shown.

Referring to Figure 6, the wind and waves will propagate from left to right in this image. With a 0° heading, the wind and waves travel in the $+x$ direction, both in regard to the global and local coordinate systems. $+z$ is up, and the y -direction follows the right-hand rule.

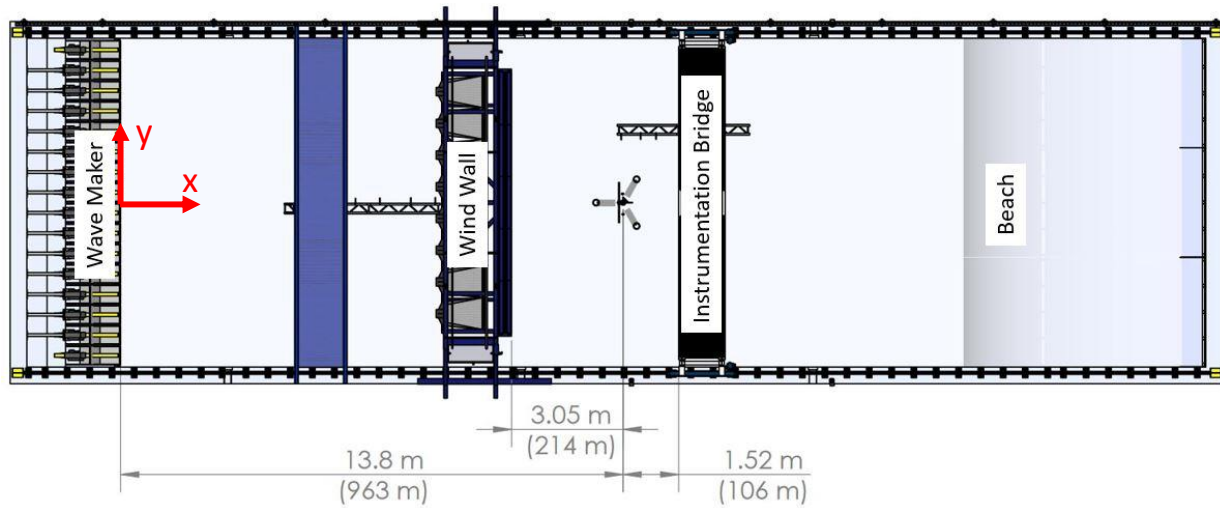


Figure 6: General Basin Layout for Campaign 4

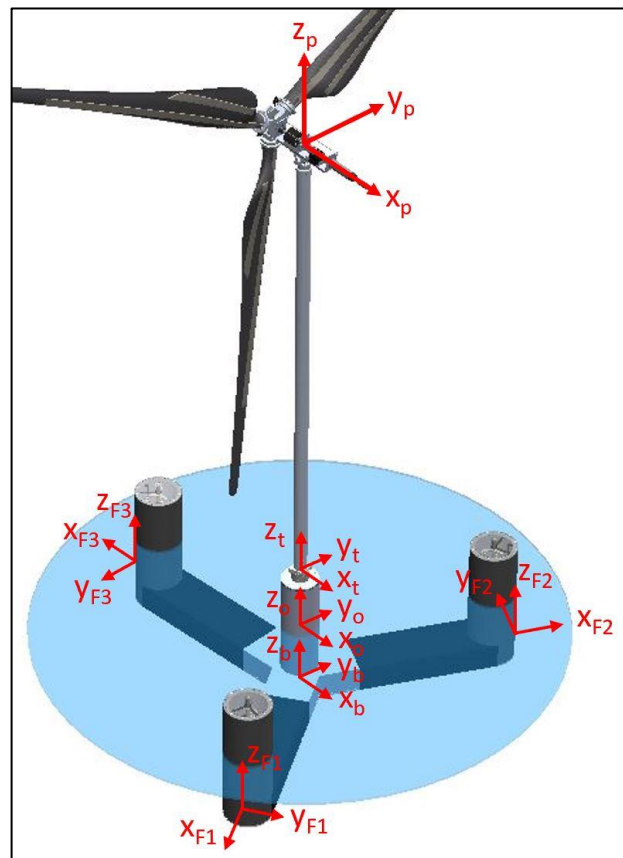


Figure 7: Location of the Hull, Tower Base, Tower Top, and Fairlead Coordinate Systems

Table 1: Axis Definitions (x,y,z locations relative to keel center at bottom of structure; Full Scale)

| Coord. System | Definition | Orientation | Origin X (m) | Origin Y (m) | Origin Z (m) |
|---------------|-------------------|----------------------|--------------|--------------|-----------------|
| O | Still Water Line | +X in wave direction | 0 | 0 | 20 [†] |
| B | Keel Center | +X in wave direction | 0 | 0 | 0 |
| T | Tower 6DOF | +X in wave direction | 0 | 0 | 37.88* |
| P | Tower Top | +X in wave direction | 0 | 0 | 161.89 |
| F1 | Column 1 Fairlead | Along mooring line 1 | 29.8 | -51.5 | 5.64 |
| F2 | Column 2 Fairlead | Along mooring line 2 | 29.1 | 51.5 | 5.64 |
| F3 | Column 3 Fairlead | Along mooring line 3 | -59.4 | 0.0 | 5.64 |

*The tower-bottom sensor location is 0.46 m below the tower base location.

[†]A nominal draft was used for the coordinate system. See Table 7 for actual draft.

Wave Measurement Locations

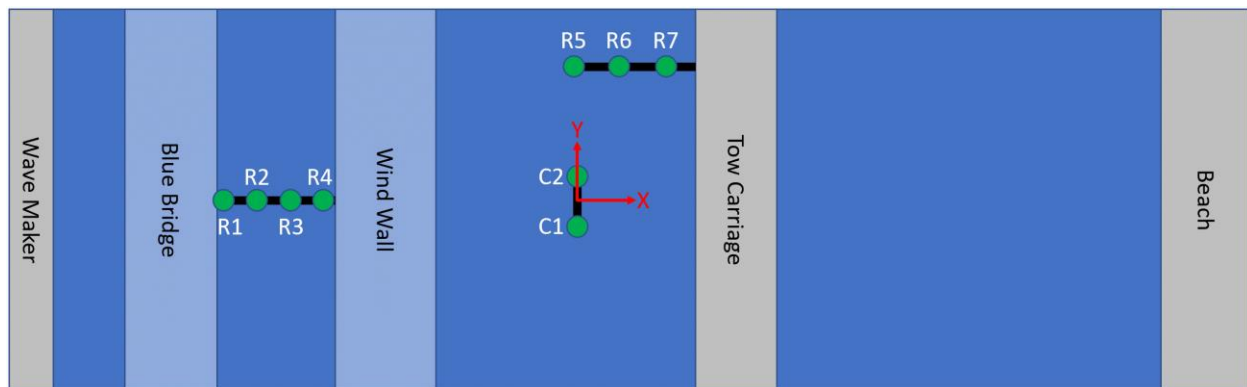


Figure 8: Basin Layout-Wave Probes (not to scale)

Table 2: Location of wave probes and anchors (relative to O coordinate system; Full Scale)

| Label | Description | X Position (m) | Y Position (m) |
|--------------|-------------------|----------------|----------------|
| Model Origin | Model Origin | 0.00 | 0.00 |
| C1 | Calibration Probe | -1.96 | -22.33 |
| C2 | Calibration Probe | -2.94 | 16.8 |
| R1 | Reference Probe | -514.64 | 1.33 |
| R2 | Reference Probe | -467.95 | 2.03 |
| R3 | Reference Probe | -408.73 | 2.73 |
| R4 | Reference Probe | -361.76 | 3.01 |
| R5 | Reference Probe | -5.6 | 127.05 |
| R6 | Reference Probe | 31.64 | 128.17 |
| R7 | Reference Probe | 61.18 | 135.52 |

3. Scaling Methodology

The Froude scaling approach that will be followed is presented here. Additional modifications that are needed are addressed in the following sections. The primary scale of the model is defined by the ratio of the full-scale (FS) to model-scale (MS) lengths. The full-scale length L_{FS} is then related to the model-scale length L_{MS} as

$$L_{FS} = \lambda L_{MS}$$

For this test program, $\lambda = 70$. This Froude scaling parameter dictates the geometric scale of the model and was selected based on maximizing the size of the model rotor within the usable area of the wind machine test area. The scaling of general quantities is provided in Table 3 in terms of the scale ratio λ . To achieve the model values, one will need to divide the full-scale values by the scale factors provided in the table. Conversely, the full-scale values will be obtained from the model data by multiplying by the scale factors noted in Table 3. The density ratio, ϕ , is 1.0, as explained in the water density mismatch section.

Table 3: Scaling parameters for Froude-scale model test campaign

| Quantity | Analytic Scale Factor |
|------------------------|-----------------------|
| Scale Factor | λ |
| Length / Position | λ |
| Velocity | $\lambda^{0.5}$ |
| Acceleration | 1 |
| Angle | 1 |
| Angular Velocity | $\lambda^{-0.5}$ |
| Angular Acceleration | λ^{-1} |
| Time | $\lambda^{0.5}$ |
| Frequency | $\lambda^{-0.5}$ |
| Mass | $\phi\lambda^3$ |
| Mass Moment of Inertia | $\phi\lambda^5$ |
| Force | $\phi\lambda^3$ |
| Moment/Torque | $\phi\lambda^4$ |

Turbine Scaling Methodology

The goal of the initial turbine design was to create a model-scale turbine that closely matched the IEA-Wind 15MW reference turbine in overall thrust and power, as well as a reasonable match in sensitivities to several key control parameters. These parameters were used as performance targets and were determined from the OpenFAST model of the IEA-Wind 15MW. Sensitivities were

obtained through linearization analysis using the frozen wake assumption and conditions specified in the turbine design. As such, the sensitivities are so called “open loop” responses since the controller action was not included in the linearization. This same process was used to quantify the performance and sensitivities of the design rotor for comparison.

With these performance targets, a Performance-Matched turbine was designed using SD7032 low-Reynolds number airfoils, adjusted blade geometry, and modified wind speed to optimize the performance match to the target turbine. The resulting turbine design was built in-house at the University of Maine's Advanced Structures and Composites Center. More information on the performance matched turbine methodology employed in this experimental program is available in publications from the group, e.g., (Kimball, et al., 2022).

Wind Speed Adjustments

In addition to modifying the blade geometry, initial design work indicated that increasing the wind speed in the basin was necessary to obtain a satisfactory performance match. Therefore, the wind speed was not simply Froude scaled, but was increased by additional 21.2%. The rotor rotational speed, however, maintained proper Froude scaling. Maintaining the proper rotor speed scaling means that we appropriately scale the 1P and 3P blade-passing frequencies, and thus their alignment with other system frequencies from the wind and waves.

As a result of the wind speed adjustment, the tip-speed ratio (TSR), which is non-dimensional, differs between the as-built design and reference IEA-Wind 15 MW reference. Thus, the TSR values for the C_p/C_t vs TSR curves are shifted between the reference and as-built designs. The as-built properties and wind speeds used in the wave tank are Froude scaled to determine their equivalent full-scale values, which is what is presented in the dataset. To compare experimental wind environments with the equivalent environments for the IEA-Wind 15MW system, one should divide the experimental wind speed 1.212 to remove the wind speed adjustment factor.

Water Density Mismatch

A complication of the scaling process presented above relates to the density of the water. At model scale, testing is performed using freshwater. However, a full-scale design will almost always be deployed in saltwater, which has a 2.5% higher density. In wave tank testing, it is typical to include this density factor in the scaling process, which affects the mass, forces, and inertia. However, the density of wind does not change between model and full scale, and therefore, adding this density factor to the forces related to wind would be inaccurate. Therefore, a new way to address the water density mismatch between scales is proposed here.

Instead of adding a scaling factor related to the difference between fresh and saltwater density, we will assume that the full-scale design will also be placed in freshwater. We would like this freshwater design to behave in a similar way as the original IEA-Wind 15 MW reference (a saltwater design) and so the following accommodations are made:

To retain the same draft, the freshwater design will decrease the mass of the system by the ratio between saltwater and freshwater density, 2.5%. Note, the center of gravity should remain at the same location.

Because the hydrostatic stiffnesses also reduce by 2.5%, the mass moments of inertia in the model are reduced by the same amount.

To keep the same balance between wind and wave forces, the “desired” thrust force will also be decreased by 2.5%.

Using this approach, the relationship between the full and model scale designs will then simply be the Froude relationship described above (with the exception of the airfoil geometry). The as-built model follows the above desired design as the goal but has some differences due to the nature of building a physical structure at scale. The sections below summarize the as-built design properties that should be modeled in this project.

4. System Properties

This section provides the relevant properties of the floating wind system needed to develop a simulation model. All information in this section is provided at the full-scale equivalent of the design using a 1:70 ratio. **It should be noted that mass and center of gravity properties of the system and its components were re-measured for Campaign 4 and, while close, are not identical to those found in the Campaign 1 and Campaign 2 reports.** An overview photo of the FOCAL system is shown in Figure 9.

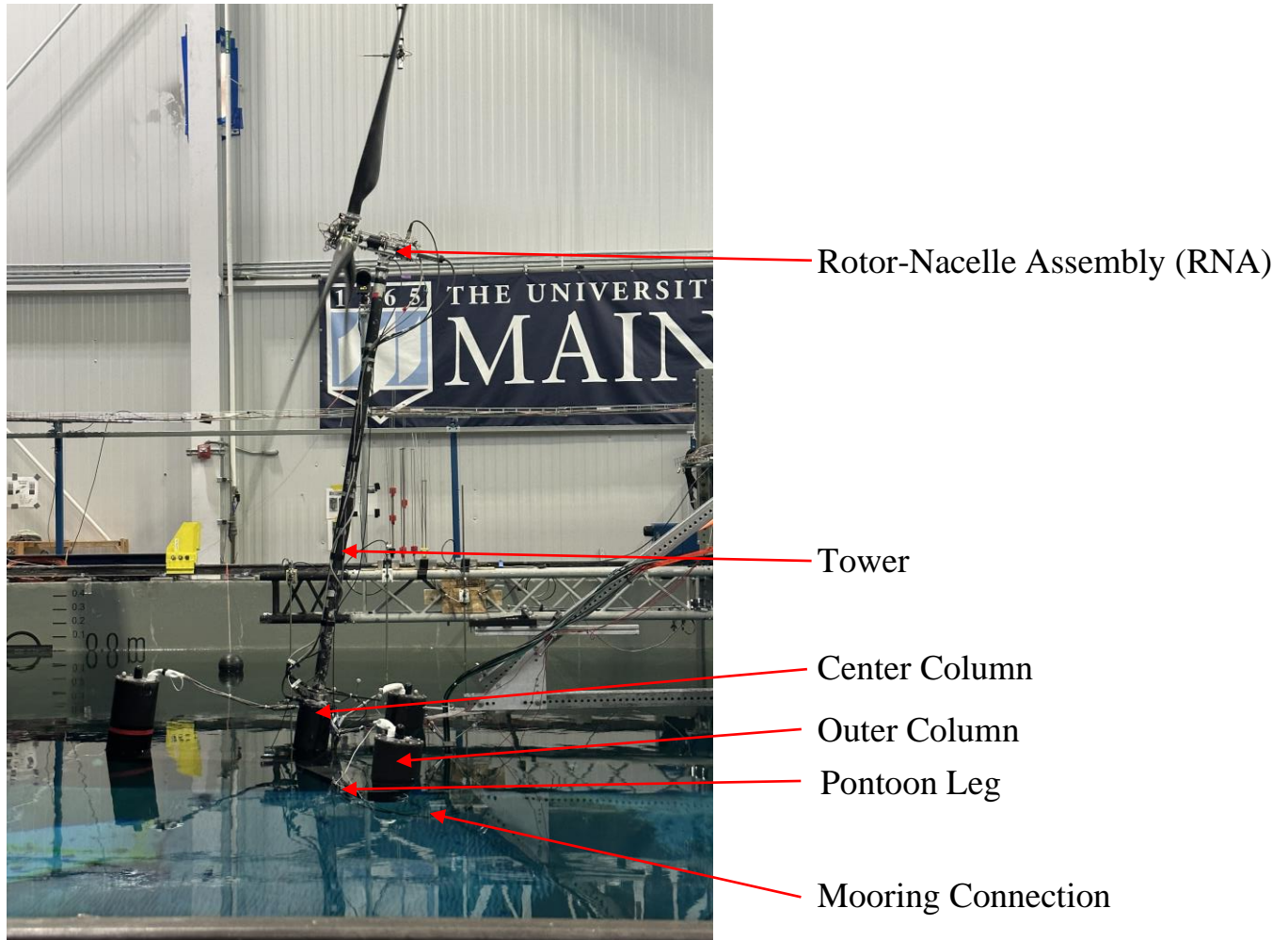


Figure 9: FOCAL Scale Model Wind Turbine and Hull

Table 4 describes the properties of the assembled system. Center of gravity locations are given relative to the centerline of the model at the bottom (keel). Inertia values are given about the system center of gravity.

Table 4: As-Built System Structural Properties

| Property | Unit | Value (Sans Umbilical) | Value (With Umbilical) |
|---|-------------------|-----------------------------------|-----------------------------------|
| Total Mass of Model | kg | 20,494,250 | 20,734,350 |
| Overall CG height from keel | m | 19.39 | 19.08 |
| Overall CG x offset keel | m | -0.08 | 0.24 |
| Overall CG y offset keel | m | -0.53 | -0.53 |
| Overall I_{xx} (Roll Inertia) about CG | kg-m ² | 4.919E+10 | 4.937E+10 |
| Overall I_{yy} (Pitch Inertia) about CG | kg-m ² | 4.936E+10 | 4.972E+10 |
| Overall I_{zz} (Yaw Inertia) about CG | kg-m ² | Not Measured | Not Measured |

Free decay results for various system configurations are shown in Table 5.

Table 5: As-Built System Free Decay Periods

| Degree of Freedom | Period (s) Sans Umbilical Fixed TMD | Period (s) With Umbilical Fixed TMD | Period (s) With Umbilical Pitch-Tuned TMD | Period (s) With Umbilical Tower-Tuned TMD |
|----------------------------------|--|--|--|--|
| Surge | 82.56 | 80.79 | - | - |
| Sway | - | 79.56 | - | - |
| Heave | 20.98 | 21.16 | - | - |
| Roll | - | 31.09 | - | - |
| Pitch | 31.00 | 30.79 | 31.23 | 30.94 |
| Yaw | - | 50.94 | - | - |

Geometric properties of the floating system are given in Table 6.

Table 6: Floating System Geometric Properties

| Dimension | Symbol | Reference Figure | Units | Value |
|--|---------------|-------------------------|--------------|--------------|
| Outer Columns Diameter | BCD | 10 | m | 12.23 |
| Outer Columns Total Height | BCH | 10 | m | 34.88 |
| Outer Column Center to Center Column Center Distance | BCC | 10 | m | 51.67 |
| Center Column Diameter | CCD | 10 | m | 9.85 |
| Center Column Total Height | CCH | 10 | m | 35.25 |
| Pontoon Leg Width | PLW | 12 | m | 12.43 |
| Pontoon Leg Height | PLH | 10 | m | 7.08 |
| Tower Diameter | TD | 10 | m | 3.57 |
| Tower Height | TH | 10 | m | 123.55 |
| Keel to Tower Base Flange Bottom | Ztb | 11 | m | 38.34 |
| Center Column Top to Tower Base Flange Bottom | HFtb | 11 | m | 3.09 |
| Keel to Fairlead | FLH | 11 | m | 5.64 |
| Hull Force Gauge Interface to Column Center | RFLEG | 11 | m | 15.05 |
| Hull Force Gauge CL to Keel | HFLEG | 11 | m | 3.51 |
| Tower Base Force Gauge Interface to Keel | HFTB | 11 | m | 37.88 |
| Tower Base Accelerometer to Keel | AccTBz | 11 | m | 37.18 |
| Nacelle Base Accelerometer to Keel | AccNBz | 10 | m | 165.23 |
| TMD Mass CG Nominal Position to Keel | RCz | 11 | m | 12.97 |
| TMD Mass CG Radial Distance to Center Column | RCx | 11 | m | 51.67 |
| Hub Height to Keel | HH | 10 | m | 169.74 |
| Rotor Diameter | RD | 14 | m | 242.8 |
| Hub Diameter | HD | 13 | m | 11.08 |
| Overhang ¹ | OH | 13 | m | 10.86 |
| Shaft Tilt | ST | 13 | deg | 6 |
| Coning Angle ² | - | - | deg | 0 |
| Tower to Shaft ³ | TTS | 13 | m | 6.715 |

¹ Overhang = horizontal distance from yaw axis to rotor apex

² Note: Model blades are rigid, coning is 0° to account for reduced blade deflection during testing.

³ Twr2Shft = vertical distance from top of tower-top flange to the rotor shaft

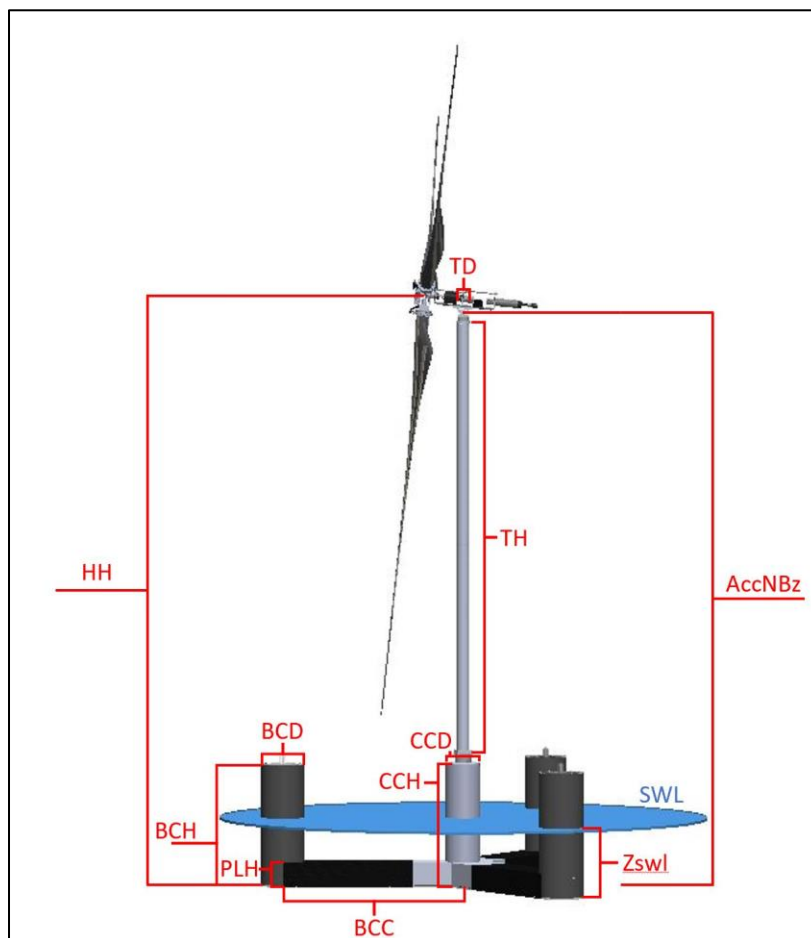


Figure 10: System Geometry Definitions

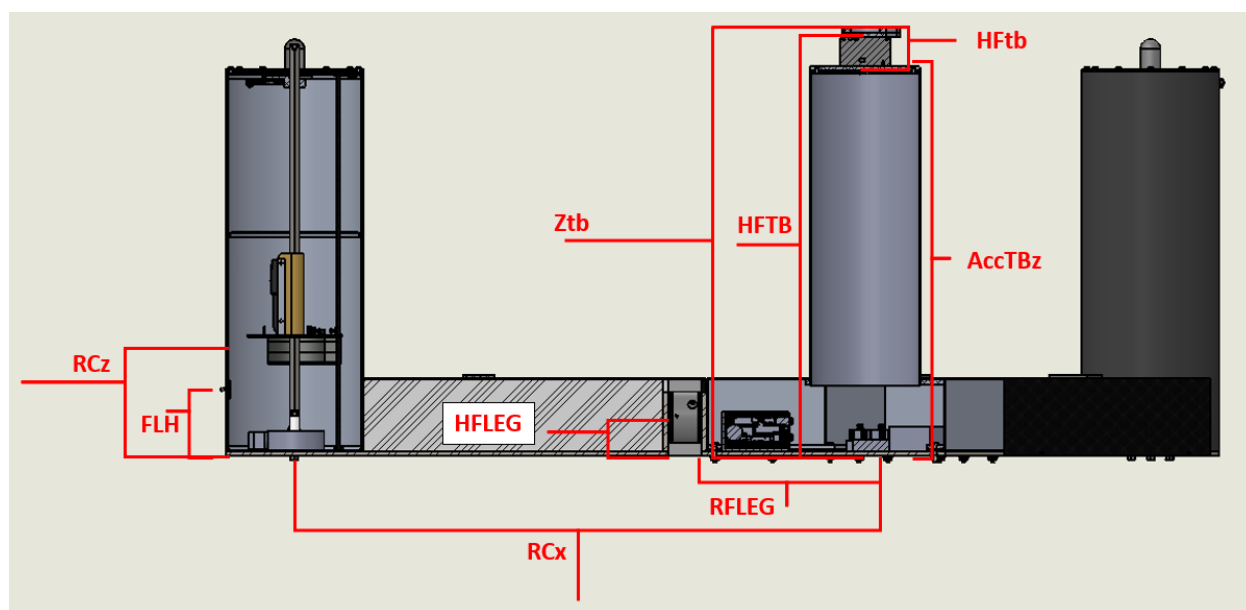


Figure 11: Hull Geometry Definitions- Side View

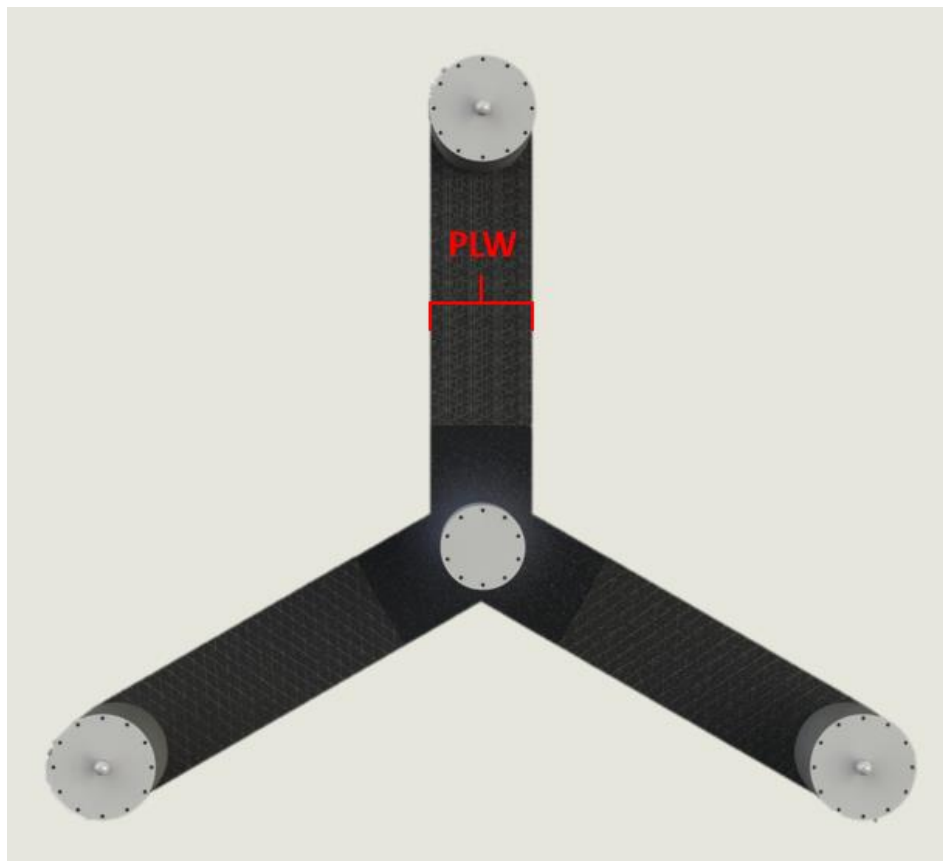


Figure 12: Hull Geometry Definitions- Top View

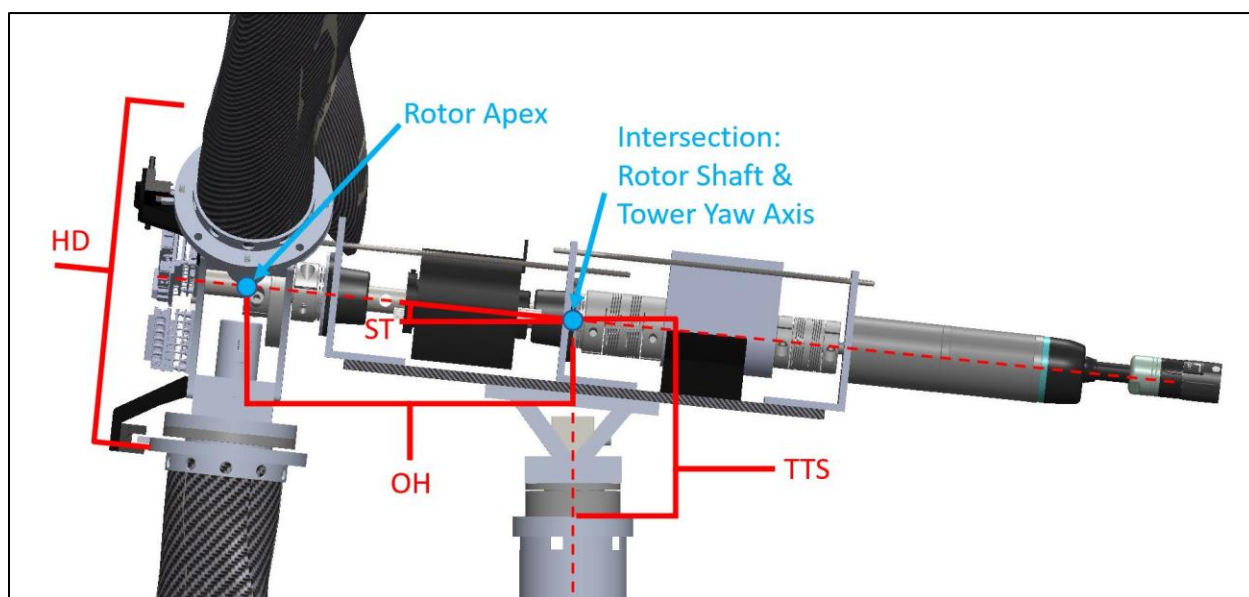


Figure 13: System Geometry Definitions- RNA Detail

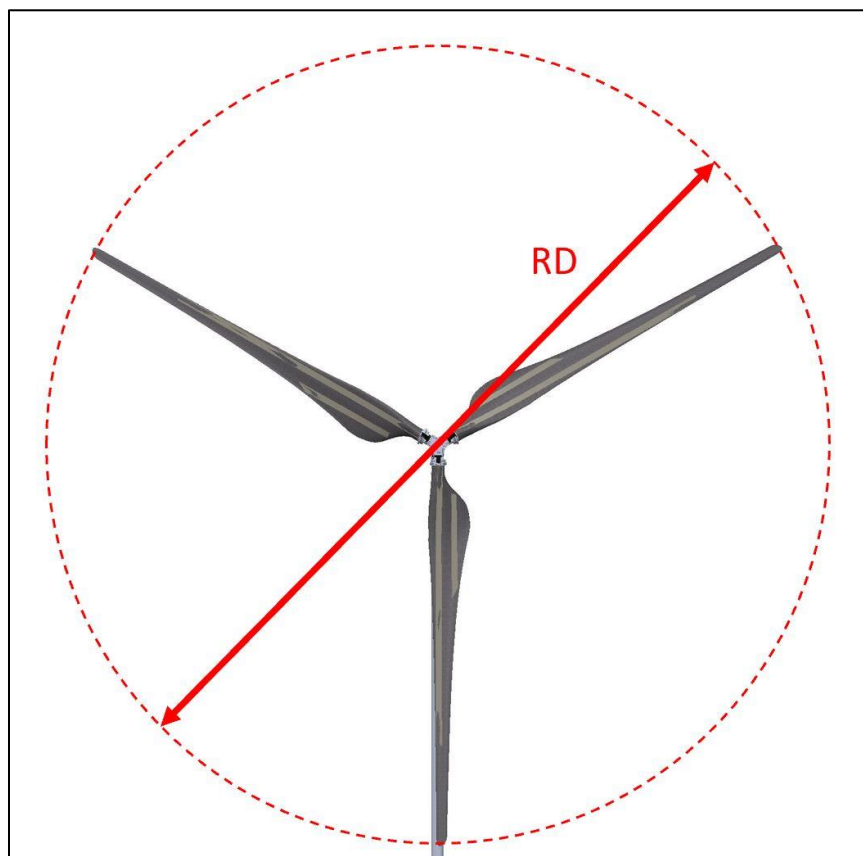


Figure 14: System Geometry Definitions- Front View

Buoyancy characteristics for the system are given in Table 7, and properties of the basin water are given in Table 8.

Table 7: Floating System Buoyancy Characteristics

| Property | Units | Value (Sans Umbilical) | Value (With Umbilical) |
|---|----------------|------------------------|------------------------|
| Draft (Keel to SWL) | m | 20.09 | 20.66 |
| Displaced volume | m ³ | 20,551.8 | 20,792.6 |
| Center of buoyancy from keel | m | 6.27 | 6.43 |
| Buoyancy force in undisplaced position ($\rho g V_0$) | N | 2.010E+08 | 2.033E+08 |

Table 8: Water Properties

| Property | Units | Value |
|---------------|-------------------|-------|
| Water depth | m | 350 |
| Water density | kg/m ³ | 997.2 |

Hull Properties

Properties for the hull are given in Table 9. The given properties represent the hull with the TMDs installed and fixed in their nominal position, but without the umbilical cable attached.

Table 9: Hull Properties

| Property | Units | Value |
|--|-------------------|--------------|
| Mass | kg | 1.866E+07 |
| Vertical Center of Gravity from keel | m | 6.94 |
| CG x offset | m | 0.08 |
| CG y offset | m | -0.60 |
| I_{xx} Roll Inertia about hull CG | kg-m ² | 1.353E+10 |
| I_{yy} Pitch Inertia about hull CG | kg-m ² | 1.402E+10 |
| I_{zz} Yaw Inertia about hull CG | kg-m ² | 1.52E+10 |
| Hydrostatic restoring in heave ($C_{33}^{Hydrostatic}$) ¹ | N/m | 4.352E+06 |
| Hydrostatic restoring in roll ($C_{44}^{Hydrostatic}$) ¹ | N-m/rad | 2.134E+09 |
| Hydrostatic restoring in pitch ($C_{55}^{Hydrostatic}$) ¹ | N-m/rad | 2.134E+09 |

¹From WAMIT model of VoltturnUS-S

Tuned Mass Damper Properties

Tuned-mass dampers (TMDs) are placed in each of the offset columns to provide damping to the system motion. Each TMD has a mass of 686,000 kg at full scale, which is accounted for in the hull properties. The spring stiffness of the TMDs are tuned to focus on either the pitch or the tower natural frequencies, and the damping was set to produce a 20% damping ratio. They are also held fixed in one location for non-control focused conditions.

Three TMD conditions were tested in the campaign:

- **Fixed:** TMD masses were held in place at their nominal position (see Table 11).
- **Pitch TMD:** TMD response was tuned to the Rigid Body Pitch Frequency of the entire floating turbine system.
- **Tower TMD:** TMD response was tuned to the 1st Tower Bending Frequency in the fore/aft direction with the entire system floating and the RNA attached

Settings for each TMD condition are outlined in Table 10. TMD center of mass information is presented in Table 11.

Table 10: Tuned Mass Damper Settings

| File Code | Target Frequency | Mass (kg) | Stiffness (N/m) | Damping (Ns/m) |
|------------------|-------------------------|------------------|------------------------|-----------------------|
| D01 | N/A (TMDs fixed) | 686,000 | inf | -- |
| D02 | Pitch | 686,000 | 31,482 | 58,783 |
| D03 | Tower | 686,000 | 4,624,376 | 712,441 |

Table 11: Tuned Mass Damper CG locations

| Position | CG Z* Location (m) |
|----------------------------|---------------------------|
| Nominal | 12.97 |
| Negative Stop Position | 2.47 |
| Positive Stop Position | 23.47 |
| <i>*Distance from Keel</i> | |

Mooring Properties

The mooring layout for the model test can be seen in Figure 15, with the locations of the attachment points given in Table 12.

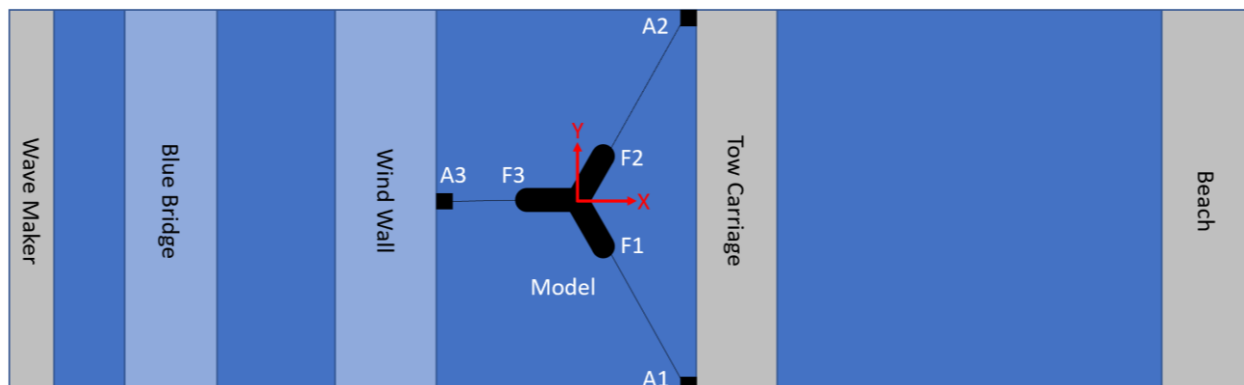


Figure 15: Mooring anchor and fairlead locations (not to scale)

Table 12: Fairlead and anchor locations

| Label | Description | X Position (m) | Y Position (m) | Z Position (m)* |
|--|----------------|----------------|----------------|-----------------|
| Origin | Model Center | 0.0 | 0.0 | 0.0 |
| A1 | Anchor Point 1 | 179.55 | -305.69 | -13.44 |
| A2 | Anchor Point 2 | 175.91 | 303.66 | -13.58 |
| A3 | Anchor Point 3 | -186.97 | 2.94 | -14.98 |
| F1 | Fairlead 1 | 29.8 | -51.5 | -14.36 |
| F2 | Fairlead 2 | 29.1 | 51.5 | -14.36 |
| F3 | Fairlead 3 | -59.4 | 0.0 | -14.36 |
| *Based of Nominal Still Water Line (Table 8) | | | | |

The moorings are fishing lines attached to spring elements, and thus can be modeled as a linear spring (see Table 13). Spring stiffnesses were set to approximate the overall surge stiffness of the VoltturnUS-S catenary mooring system under rated wind load conditions. The small diameter of the fishing wire results in minimal wave excitation to the line and will be ignored for this validation campaign. In addition to the mooring lines, a bundle of wiring related to the measurement sensors also hangs off the structure, as can be seen in Figure 16. The surge and heave stiffnesses of this umbilical bundle are included in Table 13.

Table 13: Stiffness properties of the mooring lines

| Line | Pretension (N) | Stiffness (N/m) |
|-------------------|----------------|-----------------|
| Mooring 1 (A1-F1) | 3.31E+06 | 1.26E+05 |
| Mooring 2 (A2-F2) | 3.24E+06 | 1.27E+05 |
| Mooring 3 (A3-F3) | 3.41E+06 | 1.23E+05 |
| Umbilical, Surge | - | 6.86E+03 |
| Umbilical, Heave | - | 6.22E+04 |

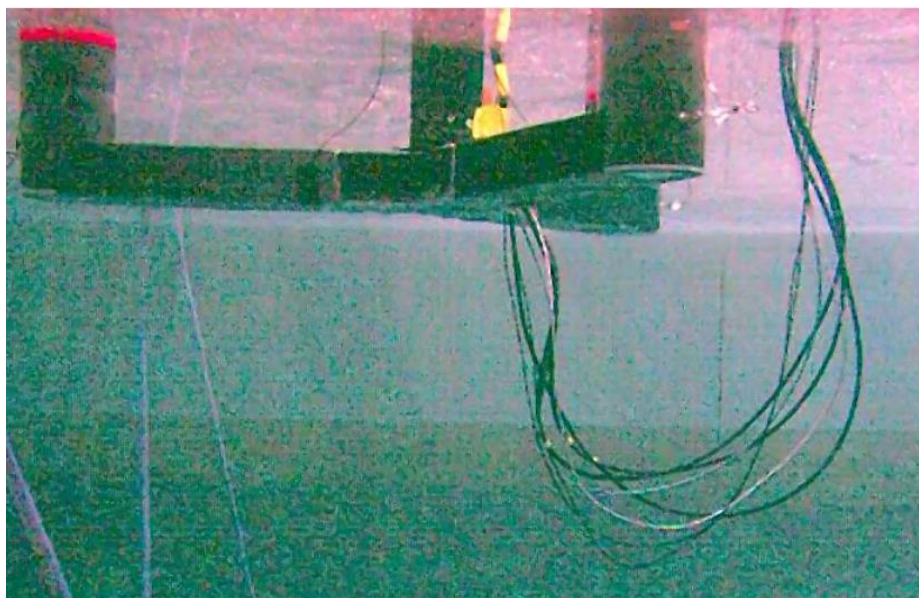


Figure 16: View of instrument cable bundle (umbilical) hanging off the hull (platform)

Mass properties for the umbilical are included in Table 14.

Table 14: Umbilical Mass Properties

| Property | Units | Value |
|----------------|-------|---------|
| Mass | kg | 240,100 |
| CG z from keel | m | -7.60 |
| CG x offset | m | 28.00 |
| CG y offset | m | 0 |

Tower Properties

The tower is a hollow aluminum tube fixed on the bottom to a force gauge and bolted on the top to the RNA. The tower flexibility is significant to the overall system dynamics and load transfer. Table 15, below, provides the relevant properties needed. A drawing of the tower and its flanges is provided in Appendix A.

Table 15: Tower Properties

| Property | Units | Value |
|---|-------------------|--------------|
| Elevation to tower base (platform top) above keel | m | 38.34 |
| Elevation to tower top (yaw bearing) above keel | m | 161.89 |
| Tower inner diameter | m | 3.36 |
| Tower outer diameter | m | 3.57 |
| E (Young Modulus) – scaled 6061 Aluminum property | GPa | 4,830 |
| E (Young Modulus) – derived to match floating frequency | GPa | 1,456 |
| G (Shear Modulus) – scaled 6061 Aluminum property | GPa | 1,281 |
| Tower mass | kg | 3.361E+05 |
| Tower + wiring mass | kg | 6.414E+05 |
| Vertical center of gravity from keel (Tower + Wiring) | m | 102.78 |
| CG x offset (Tower + Wiring) | m | 3.31 |
| CG y offset (Tower + Wiring) | m | 0.49 |
| I _{xx} Roll Inertia about tower+wiring CG | kg-m ² | 9.368E+08 |
| I _{yy} Pitch Inertia about tower+wiring CG | kg-m ² | 9.203E+08 |

The tower natural frequency was measured by striking the tower top with a hammer under several conditions. In the ‘floating’ case, the entire system is floating in the basin with the umbilical cables attached and tethered using the mooring lines. For the ‘simply supported’ case, the tower, RNA, and associated wiring are mounted to the hull, which is resting on a level floor. Average full scale natural frequencies from these tests are given in Table 16.

Table 16: Tower Natural Frequencies

| Test Condition | Average Natural Frequency (Hz) |
|--|---------------------------------------|
| Simply Supported, Fore-Aft, Fixed TMD | 0.261 |
| Simply Supported, Side-Side, Fixed TMD | 0.281 |
| Floating, Fore-Aft, Fixed TMD | 0.406 |
| Floating, Side-Side, Fixed TMD | 0.423 |
| Floating, Fore-Aft, Pitch TMD | 0.424 |
| Floating, Side-Side, Pitch TMD | 0.433 |

It is important to note that a numerical model using the scaled Aluminum material properties from Table 15 will result in a higher tower frequency than those listed in Table 16. This is due to compliance in the tower bottom load cell and the hull (Lenfest, 2023). To compensate, a derived Young’s modulus of 1,456 GPa can be used to achieve the correct floating tower frequency.

RNA Properties

The turbine used in this campaign is identical to the one used in Campaign 1, with a rated rotor speed of 7.56 RPM (full scale). Mass properties for the RNA and its components are given in Table 17. Inertia values are given about the center of gravity of the individual component. There is no CG y offset for any of the components.

Table 17: RNA Mass Properties

| Component | Mass (kg) | CG z from keel (m) | CG x offset (m) | I _{xx} about local CG (kg-m ²) | I _{yy} about local CG (kg-m ²) |
|------------------|------------------|--------------------|-----------------|---|---|
| Blades (total) | 242,633 | 169.74 | -10.86 | 6.712E+08* | 3.356E+08* |
| Hub | 442,573 | 169.72 | -10.71 | | |
| Nacelle | 479,960 | 167.73 | 4.38 | 1.580E+06 | 3.430E+07 |
| Tower-Top 6DoF | 31,899 | 162.55 | 0.00 | - | - |
| RNA Total | 1,197,065 | 168.74 | -4.40 | 6.751E+08 | 3.723E+08 |

*Rotor combined inertia expressed along rotor shaft axis (6° incline) about the combined CG of -10.76 in X and 169.73 in Z

Several other properties are useful in building a numerical model of the turbine. The nacelle yaw inertia (I_{zz}) about its center of gravity is 3.33E+07 kg-m². The hub inertia about the rotor axis is 7.34E+06 kg-m². Note that this value is included in the combined I_{xx} value for the hub and blades.

Blade Properties

The airfoils used for the scaled turbine are the Selig Donovan SD7032 airfoil, which is a low Reynolds number airfoil that achieves good performance characteristics in the Re = 100k-200k range. The blades are made from carbon fiber composite and are much stiffer than elastically scaled properties. The individual blade masses are 8.115E+04, 8.050E+04, and 8.081E+04 kg with an average mass of 8.081E+04 kg. Additional individual values are included in Appendix B: Airfoil Properties. Other structural quantities are given in Table 18 below based on the average properties for all three blades.

Table 18: Undistributed Blade Structural Properties

| Quantity | Units | Average Value | | Source |
|---|-------------------|---------------|-------------|------------|
| | | Full Scale | Model Scale | |
| <i>Length</i> ¹ | m | 1.159E+02 | 1.655 | Measured |
| <i>Blade Mass</i> | kg | 8.081E+04 | 2.356E-01 | Measured |
| <i>CM Location</i> ¹ | m | 3.773E+01 | 5.390E-01 | Measured |
| <i>First Mass Moment of Inertia</i> ¹ | kg-m | 3.049E+06 | 1.270E-01 | CAD |
| <i>Second Mass Moment of Inertia</i> ¹ | kg-m ² | 1.951E+08 | 1.161E-01 | Swing Test |

¹w.r.t. root along blade-pitch axis

The blade aerodynamic properties, including chord, twist, relative thickness, pitch axis, and airfoil information can be found in Table 19.

Table 19: As-Designed Distributed Blade Properties, 1:70 model-scale

| Radial Station | Distance along pitch axis from blade root [m] | Chord [m] | Aerodynamic twist [deg] | Aerodynamic center [% chord] | Relative thickness [%] | Airfoil ID [-] |
|-----------------------|--|------------------|--------------------------------|-------------------------------------|-------------------------------|-----------------------|
| 1 | 0 | 0.05490 | 27.13 | 50 | 100 | Cyl |
| 2 | 0.01907 | 0.05490 | 27.13 | 50 | 100 | Cyl |
| 3 | 0.27839 | 0.19800 | 13.42 | 25 | 10 | SD7032 |
| 4 | 0.33364 | 0.17409 | 11.00 | 25 | 10 | SD7032 |
| 5 | 0.38890 | 0.15515 | 9.10 | 25 | 10 | SD7032 |
| 6 | 0.44415 | 0.13981 | 7.58 | 25 | 10 | SD7032 |
| 7 | 0.49940 | 0.12716 | 6.33 | 25 | 10 | SD7032 |
| 8 | 0.55466 | 0.11657 | 5.29 | 25 | 10 | SD7032 |
| 9 | 0.60991 | 0.10758 | 4.41 | 25 | 10 | SD7032 |
| 10 | 0.66516 | 0.09986 | 3.65 | 25 | 10 | SD7032 |
| 11 | 0.72041 | 0.09316 | 3.00 | 25 | 10 | SD7032 |
| 12 | 0.77567 | 0.08729 | 2.43 | 25 | 10 | SD7032 |
| 13 | 0.83092 | 0.08211 | 1.93 | 25 | 10 | SD7032 |
| 14 | 0.88617 | 0.07751 | 1.48 | 25 | 10 | SD7032 |
| 15 | 0.94143 | 0.07339 | 1.08 | 25 | 10 | SD7032 |
| 16 | 0.99668 | 0.06969 | 0.72 | 25 | 10 | SD7032 |
| 17 | 1.05193 | 0.06633 | 0.40 | 25 | 10 | SD7032 |
| 18 | 1.10718 | 0.06329 | 0.10 | 25 | 10 | SD7032 |
| 19 | 1.16244 | 0.06051 | -0.17 | 25 | 10 | SD7032 |
| 20 | 1.21769 | 0.05796 | -0.41 | 25 | 10 | SD7032 |
| 21 | 1.27294 | 0.05562 | -0.64 | 25 | 10 | SD7032 |
| 22 | 1.32820 | 0.05346 | -0.85 | 25 | 10 | SD7032 |
| 23 | 1.38345 | 0.05146 | -1.04 | 25 | 10 | SD7032 |
| 24 | 1.43870 | 0.04960 | -1.22 | 25 | 10 | SD7032 |
| 25 | 1.49395 | 0.04788 | -1.39 | 25 | 10 | SD7032 |
| 26 | 1.54921 | 0.04626 | -1.54 | 25 | 10 | SD7032 |
| 27 | 1.60446 | 0.04476 | -1.69 | 25 | 10 | SD7032 |
| 28 | 1.65130 | 0.00498 | -1.77 | 25 | 10 | SD7032 |

5. Turbine Controller

Control of the turbine is accomplished through a real-time implementation of the National Renewable Energy Laboratory’s Reference Open Source Controller (ROSCO) (Abbas, Zalkind, Pao, & Wright, 2022). The controller is run at 120 Hz (1,000 Hz model-scale) on the cRIO-9047 real-time system utilizing the Bladed-style DISCON.IN input file. The general control strategy of ROSCO is shown in Figure 17 below, where ω_g is generator speed, τ_g is generator torque, β is blade pitch angle, v_{est} is estimated wind speed and $\Delta\omega$ is a controller set point shifting term.

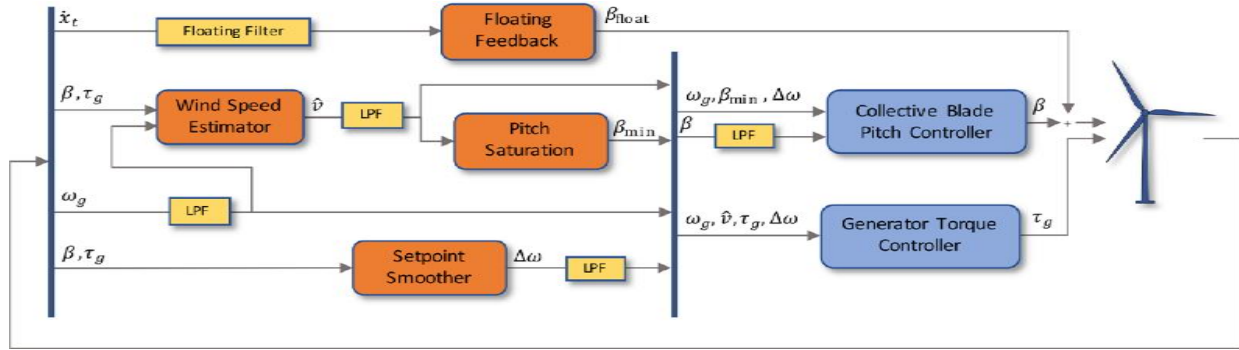


Figure 17: ROSCO general control strategy (Abbas et al., 2022)

The as-built properties of the turbine (e.g. Power, Thrust, and Torque Coefficients (C_p , C_t , and C_q), rotor inertia, and filter settings) from earlier work were used to tune the ROSCO controller using the ROSCO toolbox and the branch used by FOCAL is available on GitHub (National Renewable Energy Laboratory, 2021). Due to Reynolds number sensitivity inherent to these low Reynolds-number turbines, the velocity difference between the Rated and Above-Rated wind conditions was enough to warrant two different tunings depending on which wind environments were being considered. Measured rotor torque, rotational speed, and the current time from the experiment are passed to ROSCO at full-scale at the cRIO loop rate of 8 ms (1 ms model-scale) through the AVR-SWAP array. ROSCO then determines the appropriate blade pitch and generator torque setpoints, which are Froude-scaled down to model-scale and implemented in the experiment.

The main control loops of the “ROSCO Baseline” (RO) controller are the Collective Blade Pitch Controller and the Generator Torque Controller. For below-rated conditions, the controller uses a variable-speed generator torque controller and constant blade pitch to optimize power capture. In above-rated conditions, the baseline controller uses a proportional-integral (PI) controller to regulate rotor speed through collective blade pitch actuation. Additionally, the “Floating Feedback” (FL), “Pitch Saturation” (PS), and “Setpoint Smoother” (SS) control strategies can be toggled on/off through the DISCON.IN input file. This experiment implemented the SS for all tests and selectively activated the FL and PS control loops to assess their impact on system performance. For more information on these control options, please see (Abbas, Zalkind, Pao, & Wright, 2022). A summary of control methodologies for Campaign 4 is provided in Table 20.

Table 20: Controller strategies for FOCAL Campaign 4

| File Code | Control Method | ROSCO Tuning | Actuation | Sensing |
|------------------|-----------------------|---------------------|-------------------------------------|---|
| T01 | ROSCO Rated | Rated | Collective pitch & generator torque | Rotor speed, Generator Torque |
| T03 | ROSCO + PS | Rated | Collective pitch & generator torque | Rotor speed, Generator Torque |
| T05 | ROSCO Above Rated | Above rated | Collective pitch | Rotor speed, Generator Torque |
| T06 | ROSCO + FL | Above rated | Collective pitch | Rotor speed & nacelle acceleration from IMU |

The data provided to ROSCO's control loop are the rotor torque, measured from the inline torque transducer located on the turbine's low-speed shaft, rotor speed, measured by the rotor's encoder, and platform pitch rotational velocity measured by the hull-mounted accelerometer/inertial measurement unit (IMU). The rotor motor is coupled to the rotor and provides the ability to regulate rotor speed through application of positive or negative torque to the driveshaft. The torque setpoint calculated by ROSCO is thus implemented by controlling the rotor motor torque so that the torque measured on the torque sensor matches the setpoint provided by ROSCO. The ROSCO blade pitch setpoint is implemented via three independent servo motors in the rotor nacelle assembly (RNA) which each actuate one blade. For these experiments, the rotor was operated in collective blade pitch control and each blade was controlled to follow the blade pitch setpoint defined by ROSCO.

Floating Feedback

The FL control loop is used to decouple platform motion and generator speed variation, which occurs due to the negative damping problem in blade pitch control for floating wind turbines (Larsen & Hanson, 2007). In FOCAL, this feedback loop is considered with the Above-Rated wind and wave conditions. It uses the platform pitch rotational velocity and a tuned control loop gain to calculate a blade pitch increment, as shown in Figure 17. While ROSCO typically integrates the nacelle fore/aft acceleration or pitch rotational acceleration as the feedback signal, in FOCAL the platform pitch rotational velocity is directly available from the system instrumentation, so ROSCO is modified to take this input directly. ROSCO then filters the signal with a first-order high-pass filter and a second-order low-pass filter based on the input settings in the DISCON.IN file. The default settings were used for these filters with the high-pass frequency set to 0.0016 Hz and the low-pass frequency set to 0.034 Hz to include the system pitch natural frequency. A Bode plot of the filter is shown in Figure 18. The design of this filter is critical to the performance of the floating feedback loop as it modifies both the magnitude and phase of the feedback signal, which impacts the interaction between the blade pitch actuation and the platform global response. The platform pitch velocity is then used to compute a collective blade pitch adjustment which is added to the collective pitch signal provided by the speed regulation control loop.

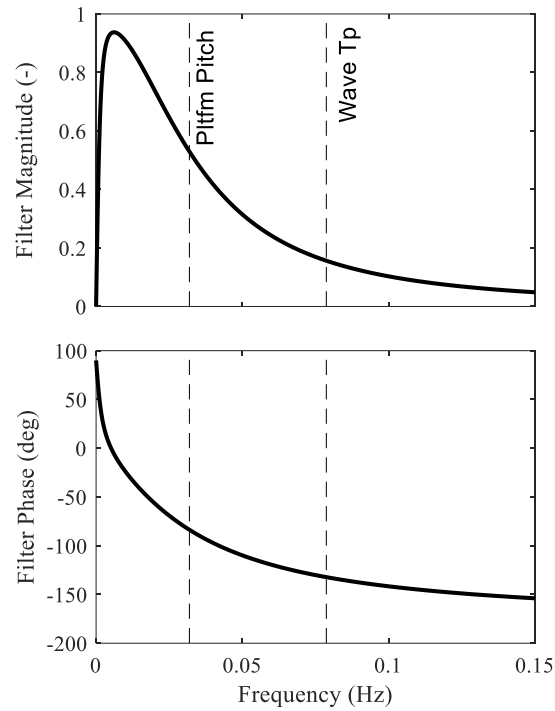


Figure 18: ROSCO FL feedback filter, magnitude and phase

Peak Shaving

Rotor thrust is typically at a maximum at near-rated turbine operation, and it plays a large role in the tower base loads experienced by the system. Peak shaving is a control strategy that reduces these loads by imposing a minimum blade pitch angle scheduled by wind speed. It is enabled by setting the “Pitch Saturation” flag in ROSCO. A maximum allowable thrust load is defined, which is then fed into a thrust coefficient (C_T) surface to determine the minimum allowable blade pitch angle at a given wind speed needed to stay under the maximum thrust (Abbas, Zalkind, Pao, & Wright, 2022). The amount of reduction in thrust must be balanced with a reduction in power output at rated, because the blades are more feathered than they would otherwise be if maximizing efficiency.

6. Instrumentation and Data Acquisition

The turbine and floating platform are fully instrumented, and all data are recorded with a National Instruments cRIO-9047 data acquisition system. Data are collected at 120 Hz (1,000 Hz model-scale) and recorded to file at 24 Hz (200 Hz model-scale). Additionally, a Qualisys motion capture system tracks reflective markers on the hull to resolve 6 degree-of-freedom (6DOF) motion of the hull. This system records data at 12 Hz (100 Hz model-scale). An overview of the system and primary instrumentation is shown in Figure 19, and a listing of sensor models used during this campaign is shown in Table 21.

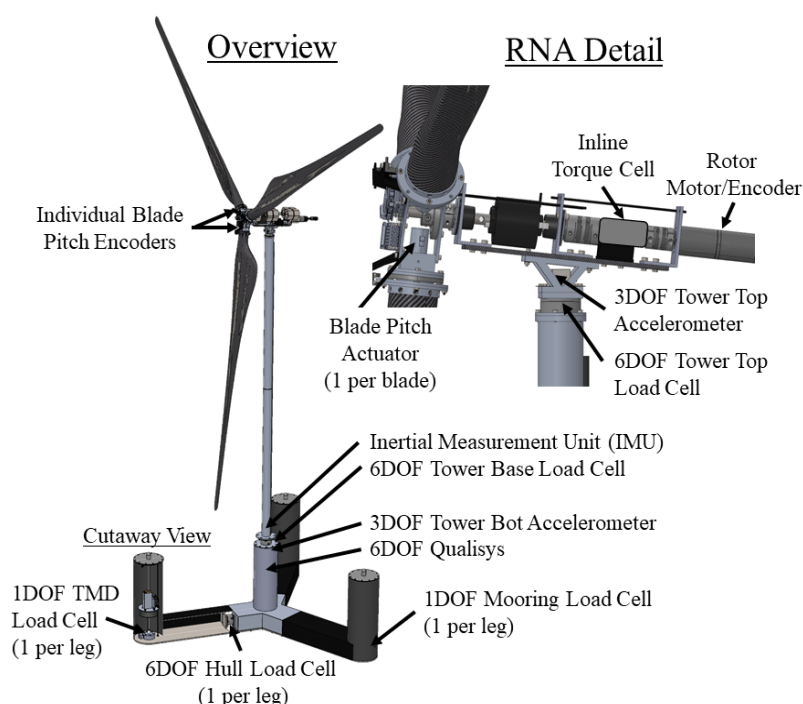


Figure 19: Instrumentation employed on the FOCAL hull and turbine

Table 21: Instruments List

| Description | Instrument | Quantity |
|--|----------------------------|----------|
| TMD load cell | Interface 2420 | 3 |
| TMD actuator | LinMot PS02-23Sx80F-HP-K | 3 |
| TMD drive | LinMot C1250-DS-XC-0S-000 | 1 |
| Pontoon internal 6DoF load cell | ATI Mini58 IP68 | 3 |
| Tower Base 6DoF load cell | ATI Mini58 IP68 | 1 |
| Tower Top 6DoF load cell | ATI Mini45 | 1 |
| Tower Top/Base Accelerometer (X, Y, Z) | PCB Piezotronics 3713F112G | 2 |
| Port/Starboard mooring load cell | Interface WMC-22N | 2 |
| Bow mooring load cell | Interface WMC-45N | 1 |
| Rotor Drive | Accelnet BEL-090-14 | 1 |

| | | |
|---------------------|---------------------------|---|
| Analog Input | Beckhoff EP3174-0002 | 2 |
| EtherCAT Junction | Beckhoff EP9128-0021 | 1 |
| Signal Conditioner | ATI 9105-ECATOEM | 5 |
| Load Cell Amplifier | Tacuna EMBSGB200 | 6 |
| DC Power Converter | CUI Inc. PQAE50-D48-S24-T | 1 |
| Leak Sensor | Grove Water Sensor | 4 |
| cRIO | cRIO-9047 | 1 |

A Note on Rotor Thrust

It is important to note that rotor thrust was not measured directly but can be calculated from the tower top 6DOF force sensor which is located between the tower top and the nacelle, see Figure 19. As such, this sensor measures all reaction loads from the nacelle. To calculate the rotor thrust force, the effect of gravity and nacelle inertial forces should be removed from the signal in post-processing using the values measured by the tower top accelerometer, the RNA mass, and the platform pitch inclination angle.

Internal Load Cells

Coordinate systems for the readings of the pontoon 6DoF internal load cells are given in Figure 20. The load cell interface location is described in Table 6. The load cell in leg 1 was found to be faulty in a previous campaign and was unable to be replaced. Its readings have been excluded from the results.

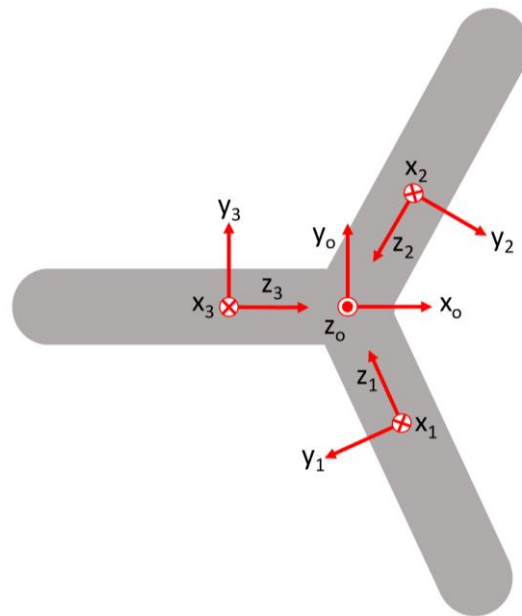


Figure 20: Internal load cell orientations (viewed from the top)

Data Post-Processing

All data was acquired and recorded in SI units at 1:70 model-scale (e.g. forces in N, torques in Nm, velocity in m/s, using the values as they are measured using the sensors in the laboratory). This dataset will be referred to as the “raw” data.

In contrast to this raw data, numerical model simulations of wind turbines tend to be at full-scale. To enable the numerical modeling community a more convenient access to the FOCAL dataset, all data was post-processed to transform the raw dataset into equivalent full-scale dimensions using Froude scaling laws as discussed in Scaling Methodology.

Other post-processing applied to the data includes:

- Time between different raw data files pertaining to the same test was synchronized and interpolated to 24 Hz (full scale).
- Wave calibration data (*waveElev*) was smoothed with a three-point moving average. This data was collected asynchronously from the rest of the test data to allow the wave probes to be placed at the equilibrium position of the model.
- Wind calibration data (*WindCal*) is the result of averaging dwell time series from two wind probes at hub height placed at the turbine centerline and at a roughly 1-m (model scale) lateral offset. This combined time series is then scaled to reflect the rotor-average wind speed determined by a survey. This data was collected asynchronously from the rest of the test data to allow the wind probes to be placed within the rotor plane area.
- The following load cell, wave probe, and accelerometer channels were de-meant by subtracting out the average value from the first ten seconds of data (full scale): *waveElev*, *accelNacelleAx*, *accelNacelleAy*, *accelNacelleAz*, *towerBotAccX*, *towerBotAccY*, *towerBotAccZ*, *towerTopFx*, *towerTopFy*, *towerTopFz*, *towerTopMx*, *towerTopMy*, *towerTopMz*, *towerBotFx*, *towerBotFy*, *towerBotFz*, *towerBotMx*, *towerBotMy*, *towerBotMz*, *leg2Fx6Dof*, *leg2Fy6Dof*, *leg2Fz6Dof*, *leg2Tx6Dof*, *leg2Ty6Dof*, *leg2Tz6Dof*, *leg3Fx6Dof*, *leg3Fy6Dof*, *leg3Fz6Dof*, *leg3Tx6Dof*, *leg3Ty6Dof*, *leg3Tz6Dof*, *waveStaff1*, *waveStaff2*, *waveStaff3*, *waveStaff4*, *waveStaff5*, *waveStaff6*, and *waveStaff7*.
- TMD position channels (*tmd1Pos*, *tmd2Pos*, and *tmd3Pos*) were referenced to the keel by adding 12.97 meters.
- *accelNacelleAy* and *towerBotAccY* were multiplied by -1 for consistency with coordinate systems.
- Blade pitch positions *pitch1Position*, *pitch2Position*, *pitch3Position*, and *pitchSetpointRosco* were converted from radians to degrees.

7. Test Program

Wind Conditions

Three wind environments were tested during Campaign 4; a gust case with sudden ramps between below-rated and near-rated operating conditions (W01, mean wind speeds of 10.10 and 12.90 m/s), a turbulent wind environment at near-rated conditions (W02, mean wind speed 12.76 m/s), and a turbulent wind with an above-rated mean wind speed (W03, mean wind speed 24.05 m/s).

Wind calibration dwell measurements of these environments were taken at the hub center, and at hub height at a roughly one meter (model scale) lateral offset. To compensate for nonuniformity in the wind field, provided wind calibration data is the result of averaging data from these two probes, and then multiplying the resultant time series by a constant to reflect a rotor-average wind speed determined by a wind survey. The processed wind calibration time series are shown in Figure 21-Figure 23. Power spectral density plots for W02 and W03 use data from 2000-12800 seconds (three hours).

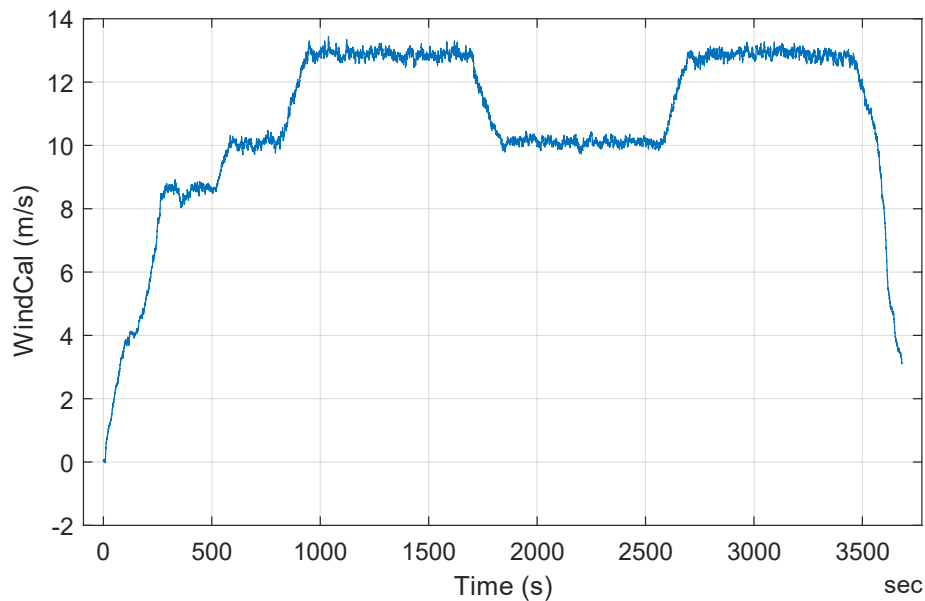


Figure 21: W01 wind calibration time history

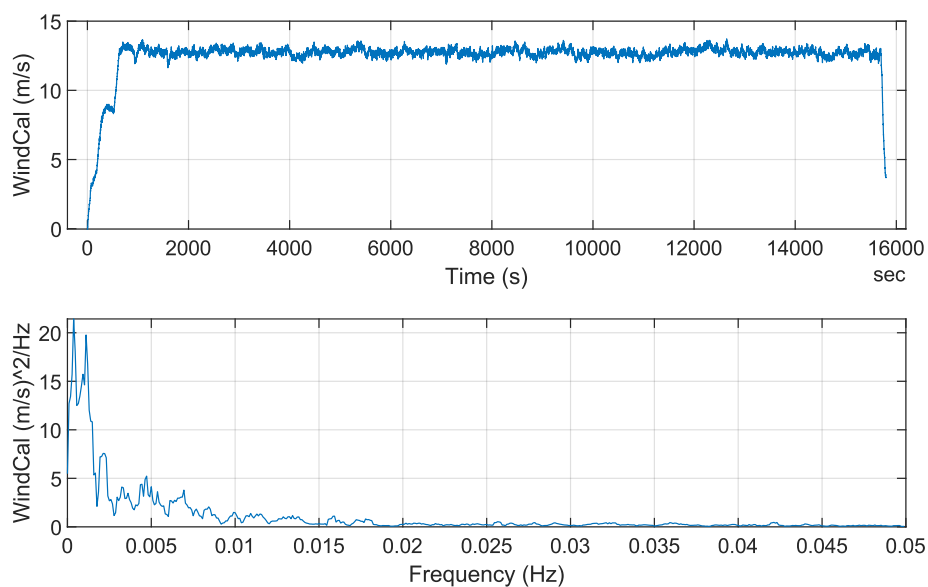


Figure 22: W02 wind calibration time history

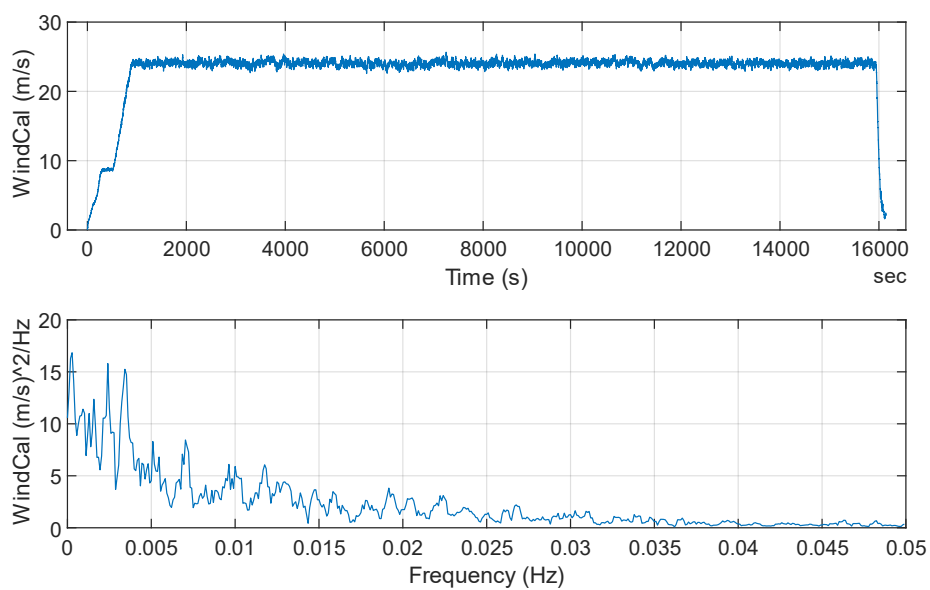


Figure 23: W03 wind calibration time history

Wave Conditions

A variety of wave conditions are used in the experimental campaign. Specifications for these waves are given in the following tables at full scale. A pink noise wave environment, specified in Table 22, was used to evaluate the response of the system over a broad range of frequencies.

Table 22: Pink noise wave properties

| Wave ID | H_s (m) | Frequency Range (Hz) |
|----------------|--------------------------|-----------------------------|
| E30 | 8.1 | 0.02 – 0.10 |

A regular wave, the properties of which are given in Table 23, was used to verify the system's response to first-order wave loads.

Table 23: Regular wave case properties

| Wave ID | H_s (m) | T_p (s) |
|----------------|--------------------------|--------------------------|
| E02 | 10.85 | 13.5 |

Two JONSWAP spectra irregular wave cases were examined: an operational sea state (E11-E15) and 1-year extreme sea states corresponding to rated wind conditions (E21-E25). Five seeds of each wave environment (different time histories with the same overall statistics) were generated to assess the dependence of measurements on individual wave time histories. Specifications for these environments are given in Table 24.

Table 24: Irregular wave case properties

| Wave ID | H_s (m) | T_p (s) | γ (-) |
|----------------|--------------------------|--------------------------|--------------|
| E11-E15 | 3.1 | 8.96 | 1.80 |
| E21-E25 | 8.1 | 12.8 | 2.75 |

The following figures show wave elevation time series captured with element 2 of the calibration probe. Power spectral density plots denote the natural surge, pitch, and floating tower frequencies for the system with a fixed TMD and the umbilical connected. PSDs were taken from t=1000-1600 seconds for E02, and from t=2000-8000 seconds for all other environments.

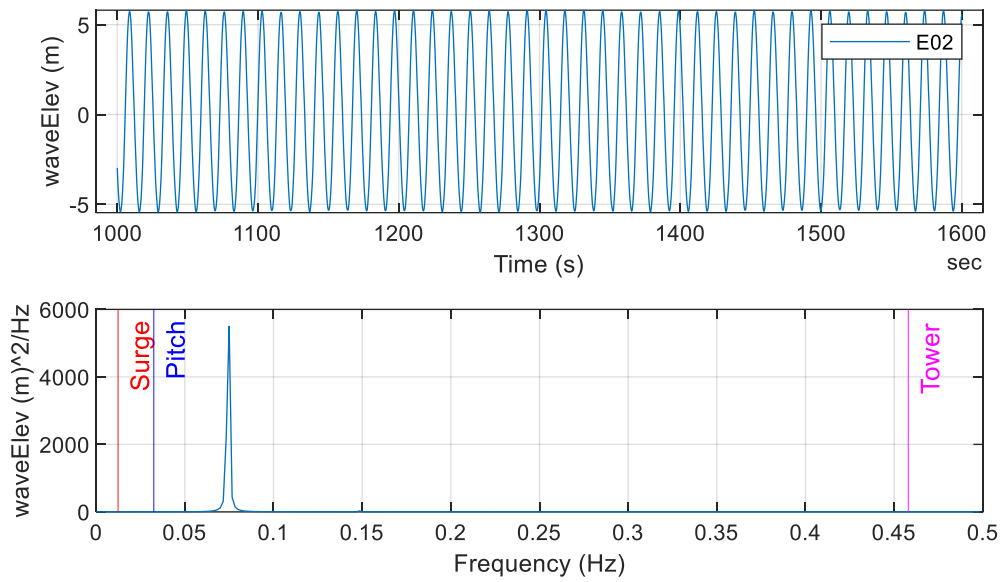


Figure 24: E02 wave calibration time history and PSD

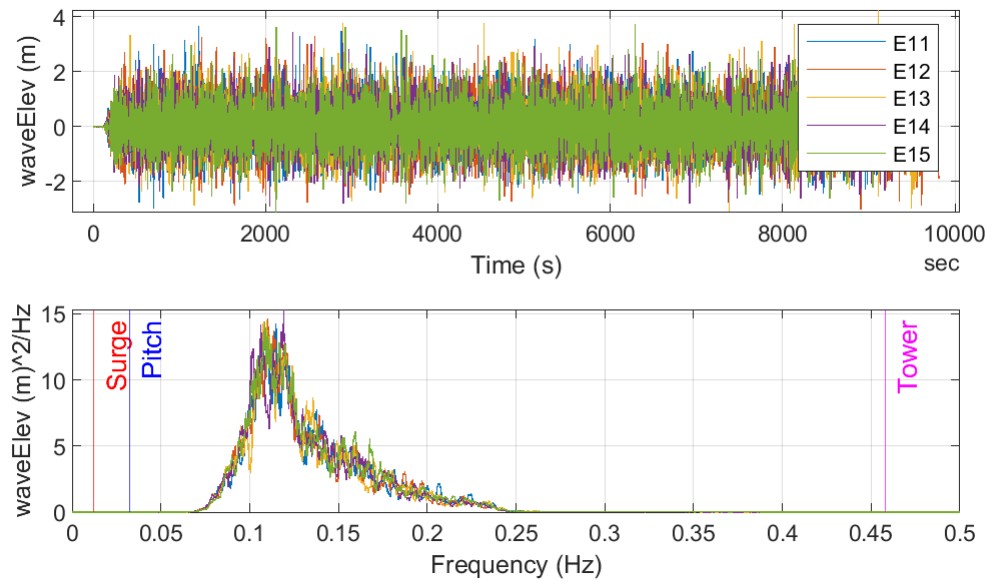


Figure 25: E11-E15 wave calibration time history and PSD

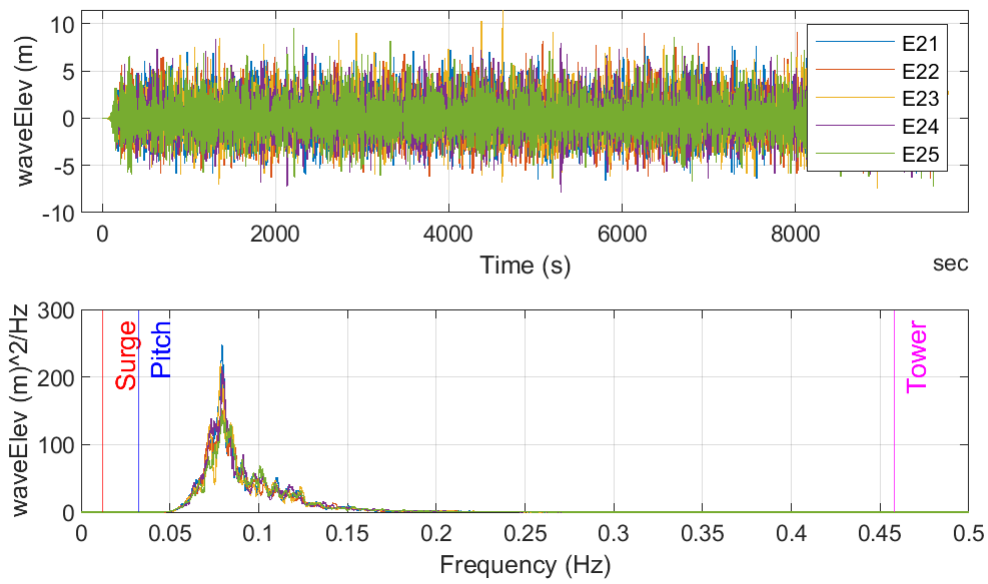


Figure 26: E21-E25 wave calibration time history and PSD

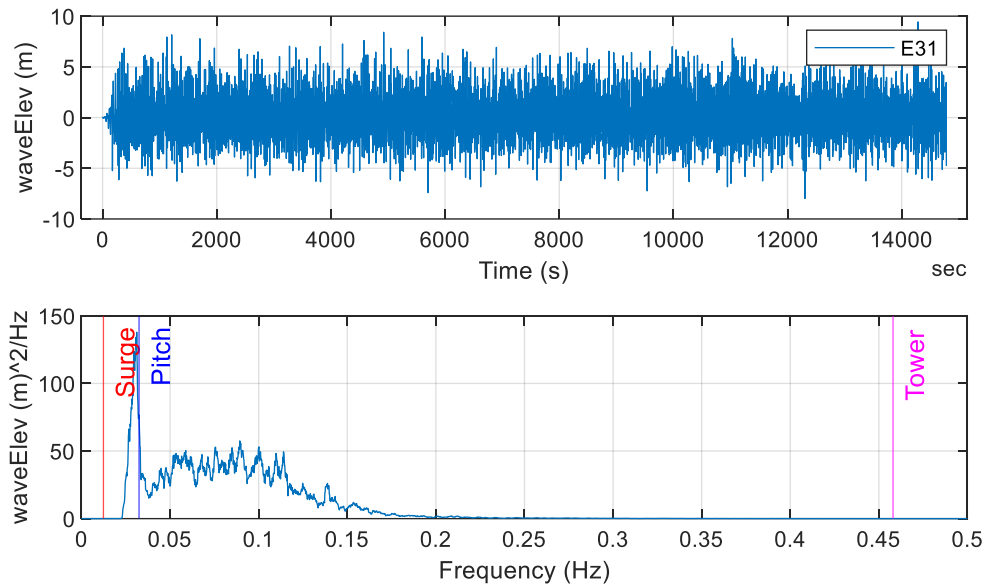


Figure 27: E30 wave calibration time history and PSD

Test Matrices

A matrix of system ID tests is provided in Table 25. Free decay tests were run by manually offsetting the model in the specified degree of freedom, then releasing and allowing the system to return to rest. Hammer tests were run by striking the tower top with the system either resting on a concrete floor (simply supported) or floating. For hydrostatic stiffness tests, a known force (heave) or moment (pitch) was applied to the model, and the displacement recorded. Mooring offset tests were run by displacing the model in surge and sway, and recording the amount of force in each mooring line to determine the stiffness.

In the following tables, codes are used to denote the test configuration. For the mooring code, “M00” denotes a test run without any mooring lines attached to the model. For “M02”, the lines are attached (though this does not indicate the status of the umbilical, which is specified separately). Tuned mass damper configuration (“D##”) follows the settings outlined in Table 10, and the turbine controller (“T##”) codes are outlined in Table 20.

Table 25: System ID Test Matrix

| Test | Description | Configurations | Repeats |
|-------------|---|--------------------------|----------------|
| FD01 | Surge Free Decay | M02D00T00 (No Umbilical) | 4 |
| | | M02D01T00 | 4 |
| FD02 | Pitch Free Decay | M02D00T00 (No Umbilical) | 4 |
| | | M02D01T00 | 4 |
| | | M02D01T05_E00W03 | 1 |
| | | M02D01T06_E00W03 | 1 |
| | | M02D02T00 | 4 |
| | | M02D02T05_E00W03 | 1 |
| | | M02D02T06_E00W03 | 1 |
| | | M02D03T00 | 4 |
| | | M02D03T05_E00W03 | 1 |
| | | M02D03T06_E00W03 | 4 |
| FD03 | Yaw Free Decay | M02D01T00 | 4 |
| FD04 | Heave Free Decay | M02D00T00 (No Umbilical) | 4 |
| | | M02D01T00 | 4 |
| FD05 | Sway Free Decay | M02D01T00 | 4 |
| FD06 | Roll Free Decay | M02D01T00 | 4 |
| HB01 | Fore/Aft Hammer Test, Simply Supported | M00D01T00 | 3 |
| HB02 | Side/Side Hammer Test, Simply Supported | M00D01T00 | 3 |
| HF01 | Fore/Aft Hammer Test, Floating | M00D01T00 | 3 |
| | | M00D02T00 | 3 |
| HF02 | Side/Side Hammer Test, Floating | M00D01T00 | 3 |
| | | M00D02T00 | 3 |
| SH01 | Hydrostatic Heave | M00D00T00 (No Umbilical) | 2 |
| | | M00D01T00 | 2 |
| SI01 | Hydrostatic Pitch | M00D00T00 (No Umbilical) | 2 |
| | | M00D01T00 | 2 |

| | | | |
|------|------------------------|--------------------------|---|
| SO01 | Static Offset: Surge + | M02D00T00 (No Umbilical) | 2 |
| | | M02D01T00 | 2 |
| SO02 | Static Offset: Surge - | M02D00T00 (No Umbilical) | 2 |
| | | M02D01T00 | 2 |
| SO03 | Static Offset: Sway + | M02D01T00 | 2 |
| SO04 | Static Offset: Sway - | M02D01T00 | 2 |

For the active wave/wind environments, testing was conducted with and without the umbilical. The matrix of tests conducted without the umbilical is shown in Table 26, and the with-umbilical matrix is presented in Table 27. Codes for the wave (“E##”) and wind (W##”) environments are specified in the previous sections of this chapter.

Table 26: No-Umbilical Test Matrix

| Environment | Repeats |
|-------------|---------|
| E02W00 | 1 |
| E11W00 | 2 |
| E12W00 | 1 |
| E13W00 | 1 |
| E14W00 | 1 |
| E15W00 | 1 |
| E21W00 | 4 |
| E22W00 | 1 |
| E23W00 | 1 |
| E24W00 | 1 |
| E25W00 | 1 |
| E30W00 | 2 |

Table 27: With-Umbilical Test Matrix

| Turbine Controller | D01 (Fixed TMD) | | D02 (Pitch-tuned TMD) | | D03 (Tower-tuned TMD) | |
|-----------------------|-----------------|---------|-----------------------|---------|-----------------------|---------|
| | Environment | Repeats | Environment | Repeats | Environment | Repeats |
| T00 | E02W00 | 1 | | | | |
| | E11W00 | 5 | | | | |
| | E12W00 | 1 | | | | |
| | E13W00 | 1 | | | | |
| | E14W00 | 1 | E02W00 | 1 | E02W00 | 1 |
| | E15W00 | 1 | E11W00 | 1 | E11W00 | 1 |
| | E21W00 | 5 | E21W00 | 1 | E21W00 | 1 |
| | E22W00 | 1 | E30W00 | 1 | E30W00 | 1 |
| | E23W00 | 1 | | | | |
| | E24W00 | 1 | | | | |
| | E25W00 | 1 | | | | |
| | E30W00 | 5 | | | | |

| | | | | | | |
|-----|--------|---|------------------|--------|--------|---|
| T01 | E00W01 | 1 | E30W02 | 1 | | |
| | E00W02 | 1 | | | | |
| | E02W01 | 1 | | | | |
| | E11W02 | 4 | | | | |
| | E12W02 | 1 | | | | |
| | E13W02 | 1 | | | | |
| | E14W02 | 1 | | | | |
| | E15W02 | 1 | | | | |
| | E30W02 | 1 | | | | |
| T03 | E00W01 | 1 | E11W02 | 4 | E11W02 | 1 |
| | E02W01 | 1 | E12W02 | 1 | E12W02 | 1 |
| | E30W02 | 1 | E15W02 | 1 | E13W02 | 1 |
| | | | E30W02 | 5 | E14W02 | 1 |
| | | | | | E30W02 | 5 |
| T05 | E00W03 | 1 | E02W03 E21W03 | 1 1 | E02W03 | 1 |
| | E02W03 | 1 | | | | |
| | E21W03 | 5 | | | | |
| | E22W03 | 1 | | | | |
| | E23W03 | 1 | | | | |
| | E24W03 | 1 | | | | |
| | E25W03 | 1 | | | | |
| T06 | E02W03 | 1 | E02W03 | 1 | E02W03 | 1 |
| | E21W03 | 1 | E21W03 | 5 | E21W03 | 1 |
| | | | | | E22W03 | 1 |
| | | | | | E24W03 | 1 |
| | | | | | E25W03 | 1 |

As an important note regarding Table 27, it was noticed during post-processing that the repeatability characteristics of the wind field caused slight differences in ROSCO's wind speed estimate for some runs at rated wind (W02). Because of the characteristics of the blade pitch controller at this transition region, runs with the slightly lower wind estimate saw much less blade pitch actuation. An example is shown in Figure 28.

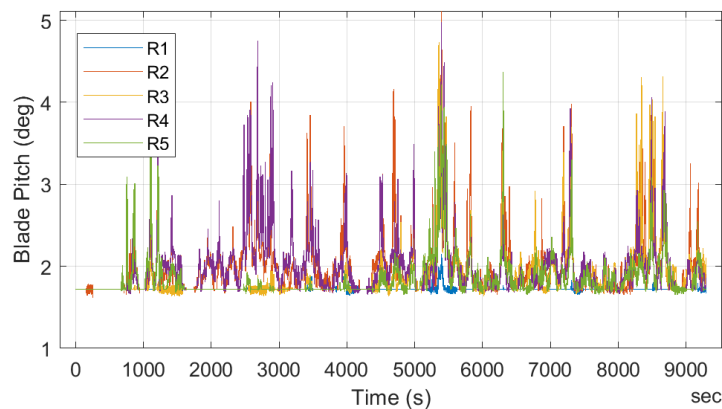


Figure 28: M02D02T03 E11 Repeats Blade Pitch Actuation

Table 28 categorizes the runs of DLC 1.2 based on the amount of blade pitching observed. Runs listed at “Low Throughout” were excluded from the tally of repeats in Table 27.

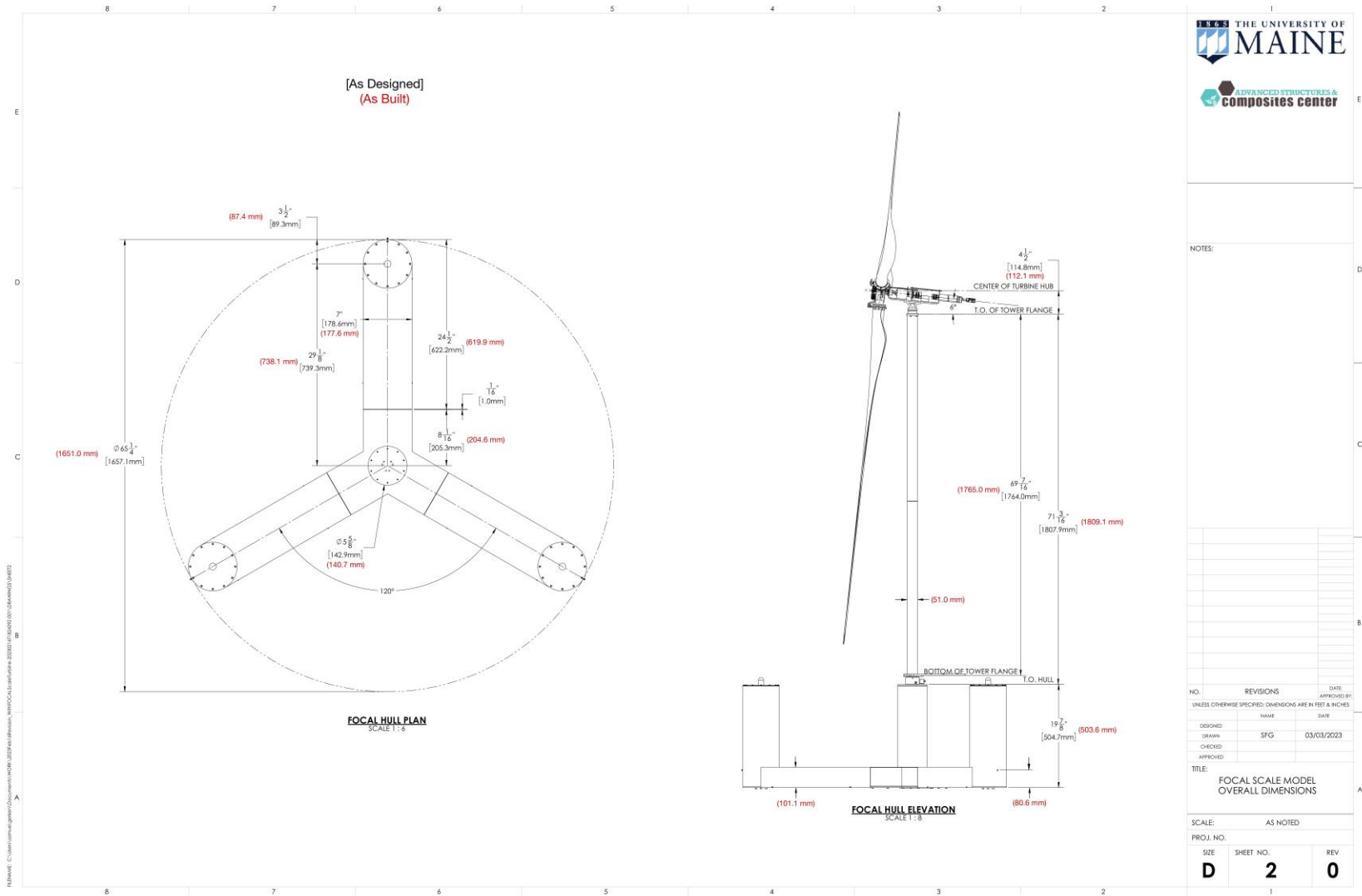
Table 28: DLC 1.2 Test Validity

| Test | Amount of Blade Pitching | | |
|---------------------------|--------------------------|----------------|----------------|
| | As Expected | Subset t= | Low Throughout |
| M02D01T01_AC01_E11W02_R01 | X | | |
| M02D01T01_AC01_E11W02_R02 | | | X |
| M02D01T01_AC01_E11W02_R03 | X | | |
| M02D01T01_AC01_E11W02_R04 | X | | |
| M02D01T01_AC01_E11W02_R05 | | 3800:9300(end) | |
| M02D01T01_AC01_E12W02_R01 | | 2000:9500(end) | |
| M02D01T01_AC01_E13W02_R01 | X | | |
| M02D01T01_AC01_E14W02_R01 | X | | |
| M02D01T01_AC01_E15W02_R01 | X | | |
| M02D01T03_AC01_E11W02_R01 | | | X |
| M02D02T01_AC01_E11W02_R01 | | | X |
| M02D02T03_AC01_E11W02_R01 | | | X |
| M02D02T03_AC01_E11W02_R02 | X | | |
| M02D02T03_AC01_E11W02_R03 | | 5000:9300(end) | |
| M02D02T03_AC01_E11W02_R04 | X | | |
| M02D02T03_AC01_E11W02_R05 | | 5000:9300(end) | |
| M02D02T03_AC01_E12W02_R01 | | 5000:9300(end) | |
| M02D02T03_AC01_E13W02_R01 | | | X |
| M02D02T03_AC01_E14W02_R01 | | | X |
| M02D02T03_AC01_E15W02_R01 | | 5000:9300(end) | |
| M02D03T03_AC01_E11W02_R01 | | 5000:9300(end) | |
| M02D03T03_AC01_E11W02_R02 | | | X |
| M02D03T03_AC01_E11W02_R03 | | | X |
| M02D03T03_AC01_E11W02_R04 | | | X |
| M02D03T03_AC01_E12W02_R01 | | 4500:9300(end) | |
| M02D03T03_AC01_E13W02_R01 | X | | |
| M02D03T03_AC01_E14W02_R01 | X | | |
| M02D03T03_AC01_E15W02_R01 | | | X |

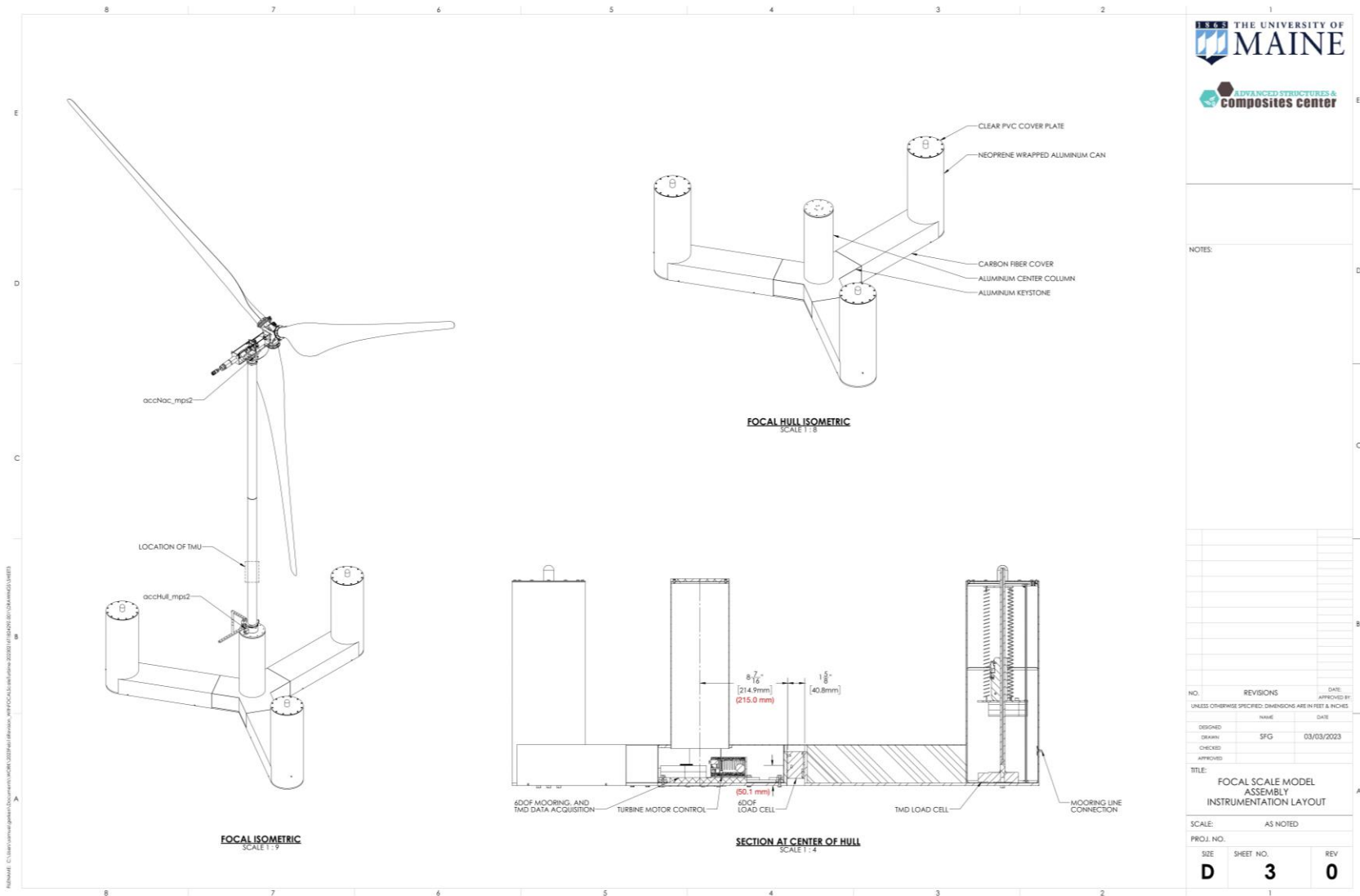
Bibliography

- Abbas, N., Zalkind, D., Pao, L., & Wright, A. (2022). A Reference Open-Source Controller for Fixed and Floating Offshore Wind Turbines. *Wind Energy Science*, 7, 53-73. Retrieved from <http://wes.copernicus.org/articles/7/53/2022>
- American Bureau of Shipping. (2013). *ABS- Guide for Building and Classing Floating Offshore Wind Turbine Installations*.
- Det Norske Veritas. (2010). *DNV-RP-C205: Environmental Conditions and Environmental Loads*.
- Fowler, M., Kimball, R., Thomas, D., & Goupee, A. (2013). Design and Testing of Scale Model Wind Turbines for Use in Wind/Wave Basin Model Tests of Floating Offshore Wind Turbines. *ASME 2013 32nd International Conference on Ocean, Offshore and Arctic Engineering*. Nantes, France.
- Gaertner, Evan et al. (2020). *Definition of the IEA 15-Megawatt Offshore Reference Turbine*. Golden, CO: National Renewable Energy Laboratory.
- International Towing Tank Conference. (2017). *00 - ITTC - Recommended Procedures and Guidelines*. Retrieved from ITTC: <https://itcc.info/media/8372/index.pdf>
- Jonkman, J., Butterfield, S., Musial, W., & Scott, G. (2009). *Definition of a 5-MW Reference Wind Turbine for Offshore System Development*. Golden, CO: National Renewable Energy Lab. (NREL). doi:10.2172/947422
- Kimball, R., Goupee, A., de Ridder, E., & Helder, J. (2014). Wind/Wave Basin Verification of a Performance Matched Scale Model Wind Turbine on a Floating Wind Turbine Platform. *ASME 33rd International Conference on Ocean, Offshore and Arctic Engineering*. San Francisco, California USA.
- Kimball, R., Robertson, A., Fowler, M., Wright, A., Goupee, A., Lenfest, E., & Parker, A. (2022). Results from the FOCAL Experiment Campaign 1: Turbine Control Co-Design. *TORQUE 2022*. Delft.
- Larsen, T. J., & Hanson, T. D. (2007). A nmethod to avoid negative damped low frequent tower vibrations for a floating, pitch controlled wind turbine. *Journal of Physics, Conference Series*.
- Lenfest, E. (2023). *Floating Offshore Wind Controls Advanced Laboratory (FOCAL) Experimental Program- Campaigns 2 and 3 Testing Summary and Data Report (Report No. 23-56-1183)*. Orono: University of Maine.
- Martin, H. (2009). *Development of a Scale Model Wind Turbine for Testing of Offshore Floating Wind Turbine Systems*. Orono, ME: University of Maine.
- National Renewable Energy Laboratory. (2021). *ROSCO Toolbox Version 2.3.0*. Retrieved from https://github.com/NREL/ROSCO_toolbox/tree/focal
- Statoil Hydro. (2008). *Hywind Metocean Design Basis: MBM-MGE-RA 32*. Statoil Hydro.
- To Be Published. (n.d.). Verification and Validation of Model-Scale Turbine Performance and Control for the IEA Wind 15 MW Reference Wind Turbine.
- Torsethaugen, K., & Haver, S. (2004). Simplified Double Peak Spectral Model for Ocean Waves. *The Fourteenth (2004) International Offshore and Polar Engineering Conference*. Toulon, France.

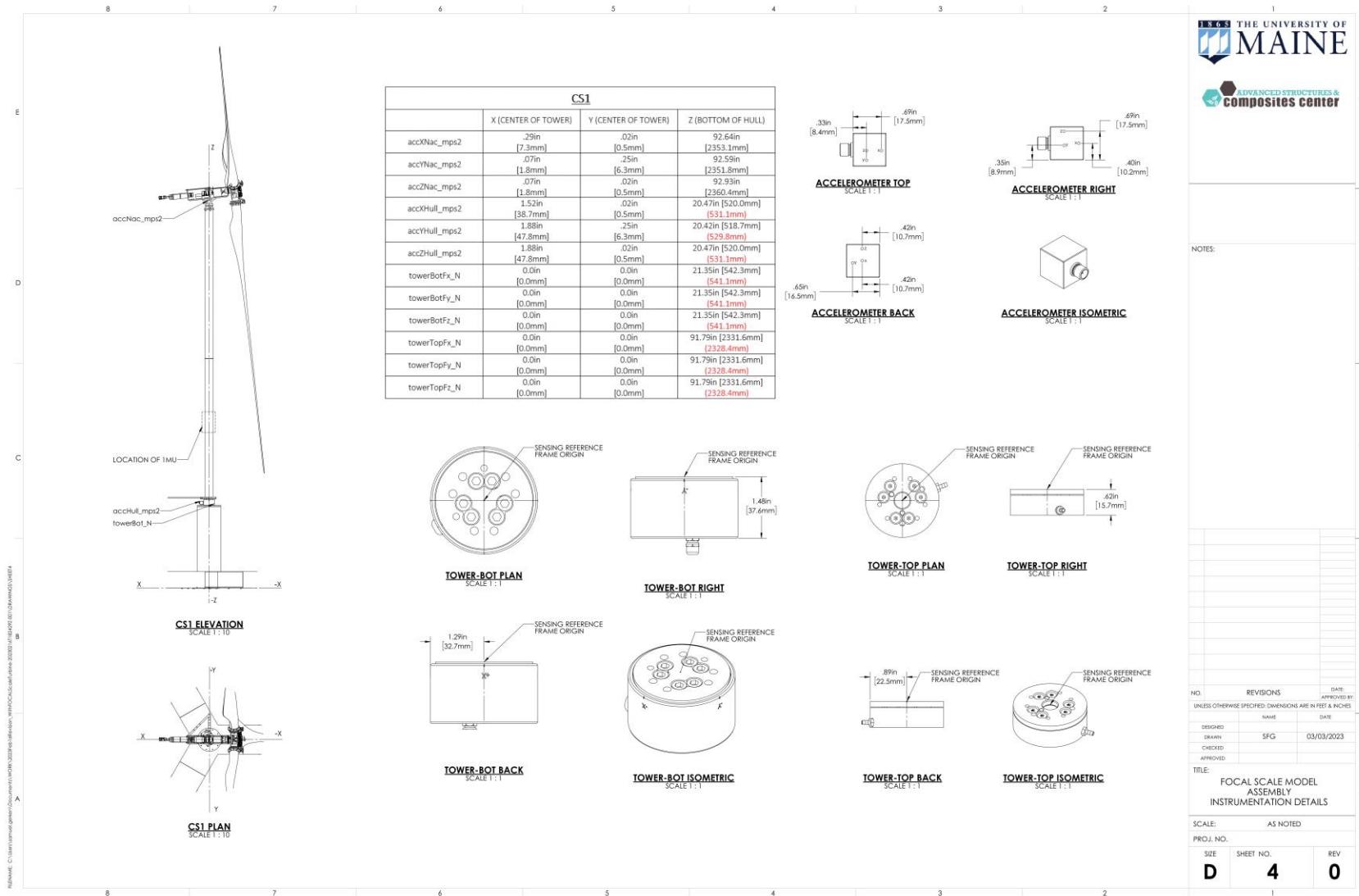
University of Maine's Advanced Structures and Composites Center
Report Number: 23-57-1183



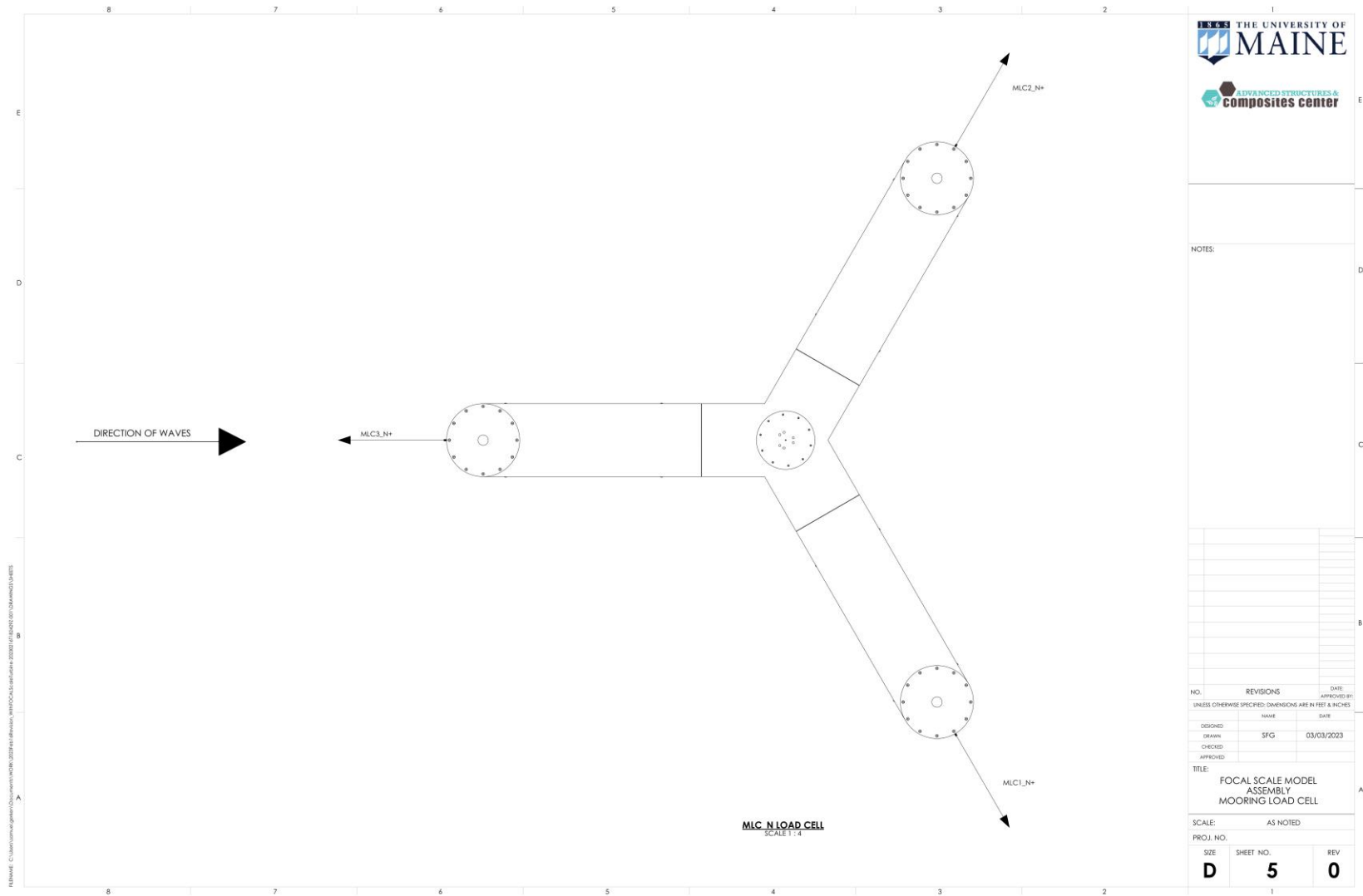
University of Maine's Advanced Structures and Composites Center
Report Number: 23-57-1183



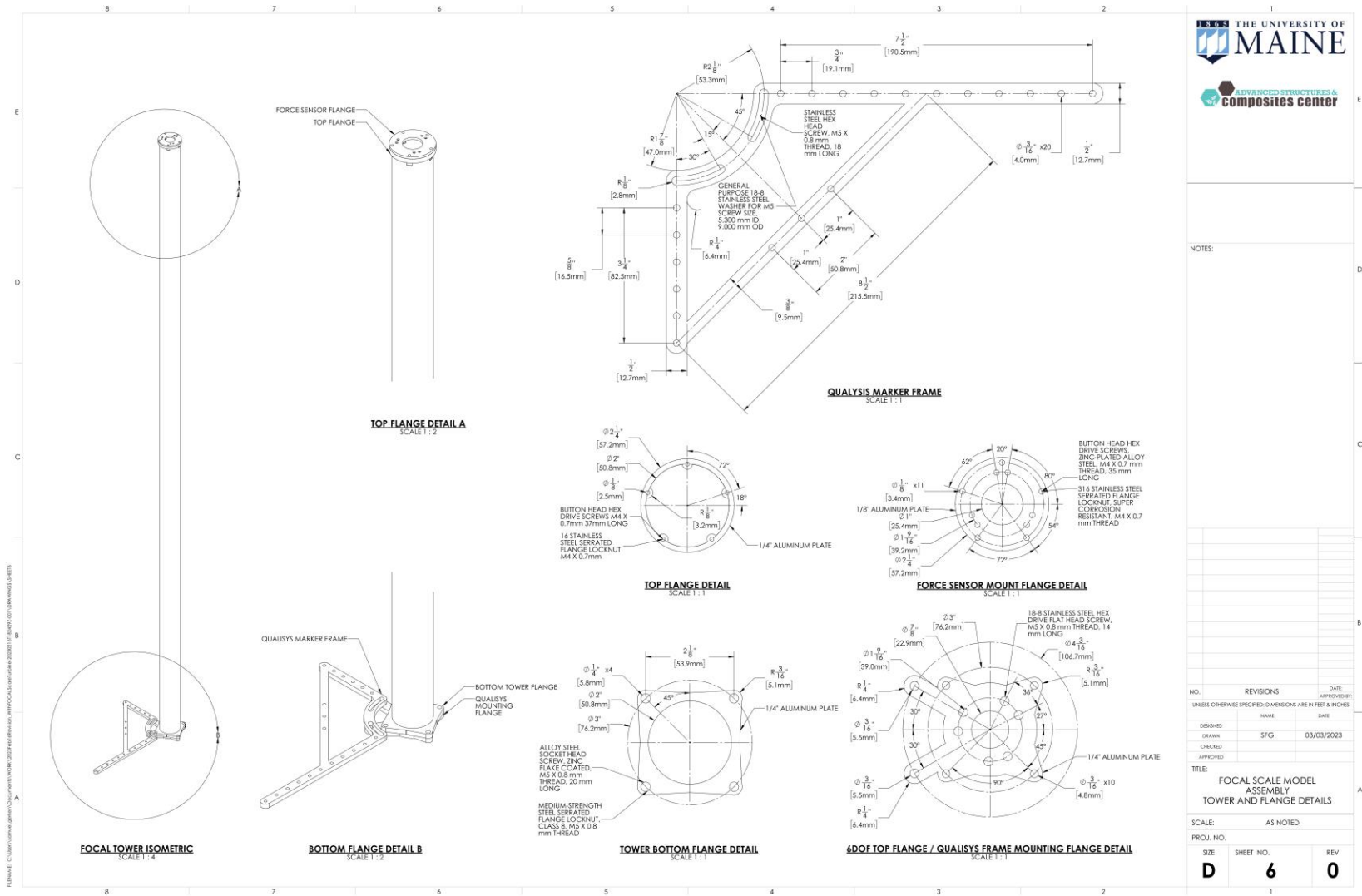
University of Maine's Advanced Structures and Composites Center
Report Number: 23-57-1183

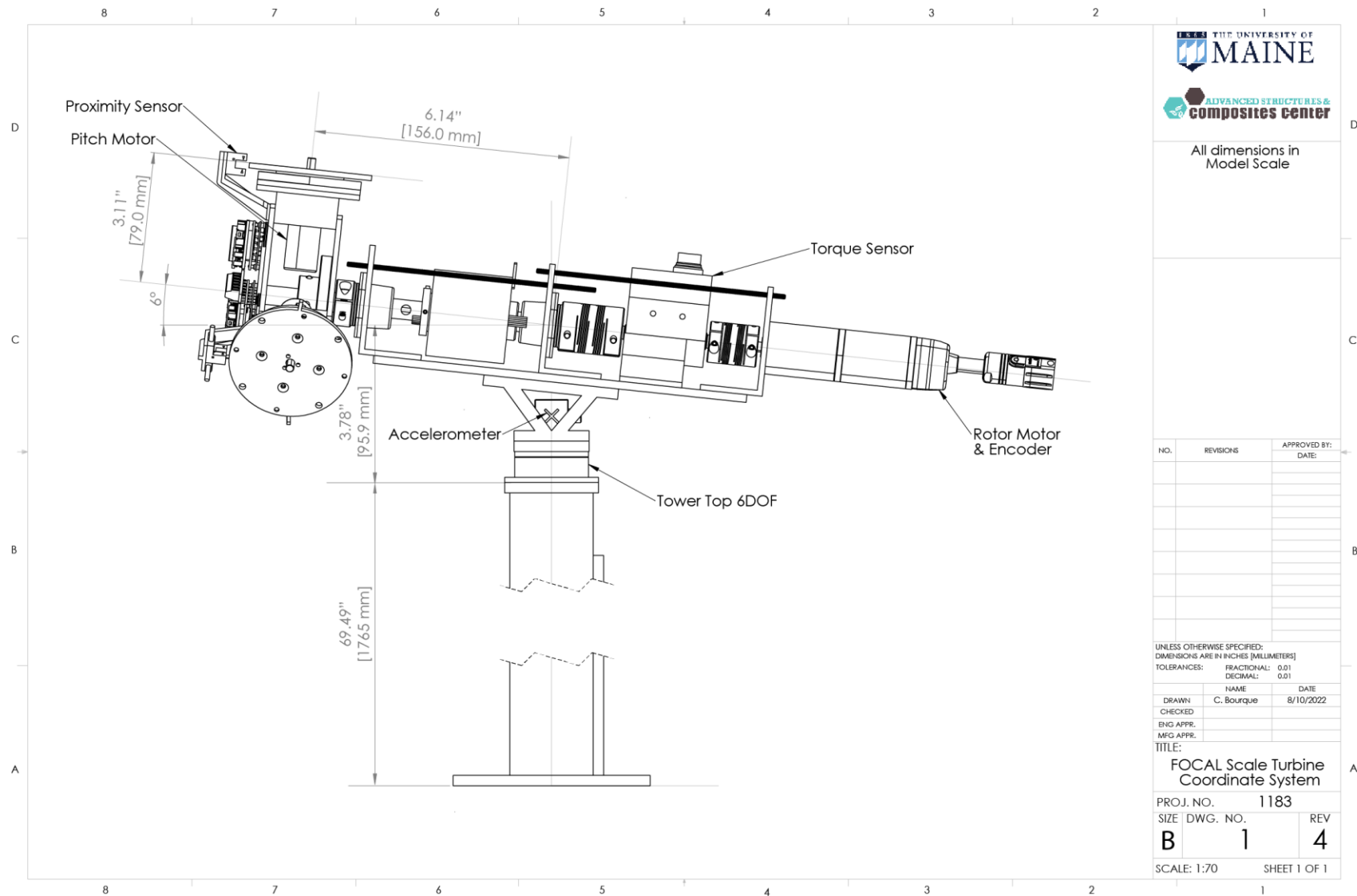


University of Maine's Advanced Structures and Composites Center
Report Number: 23-57-1183



University of Maine's Advanced Structures and Composites Center
Report Number: 23-57-1183





Appendix B: Airfoil Properties

SD7032- Rated

| α (deg) | C_l | C_d | α (deg) | C_l | C_d |
|----------------|-----------|----------|----------------|----------|----------|
| -180 | 0 | 0.031845 | 0.99971 | 0.079286 | 0.053075 |
| -178.2219 | 0.053679 | 0.033082 | 1.9812 | 0.17768 | 0.051003 |
| -176.4439 | 0.10736 | 0.036785 | 2.9917 | 0.2936 | 0.048922 |
| -174.6658 | 0.16104 | 0.042943 | 3.9736 | 0.4125 | 0.047021 |
| -172.8878 | 0.21472 | 0.051529 | 4.9818 | 0.5328 | 0.045263 |
| -171.1097 | 0.26839 | 0.062511 | 5.9906 | 0.64305 | 0.043774 |
| -169.3317 | 0.32207 | 0.075847 | 6.9725 | 0.73265 | 0.042654 |
| -167.5536 | 0.37575 | 0.091484 | 7.9826 | 0.79835 | 0.041912 |
| -165.7756 | 0.42943 | 0.10936 | 8.9649 | 0.82856 | 0.041659 |
| -163.9975 | 0.48311 | 0.12941 | 9.9771 | 0.83772 | 0.044586 |
| -162.2195 | 0.53679 | 0.15155 | 10.9612 | 0.84378 | 0.052663 |
| -160.4414 | 0.59047 | 0.1757 | 11.973 | 0.84905 | 0.065756 |
| -158.6634 | 0.64415 | 0.20176 | 12.9564 | 0.85514 | 0.082566 |
| -156.8853 | 0.67832 | 0.22964 | 13.9714 | 0.86482 | 0.10355 |
| -155.1073 | 0.69515 | 0.25921 | 14.9821 | 0.87488 | 0.12751 |
| -150.4567 | 0.69521 | 0.34377 | 15.9645 | 0.87936 | 0.15315 |
| -145.8062 | 0.67813 | 0.43693 | 17.9572 | 0.83407 | 0.21004 |
| -141.1557 | 0.64299 | 0.53621 | 19.9512 | 0.77057 | 0.26963 |
| -136.5052 | 0.60809 | 0.63897 | 24.8927 | 0.70412 | 0.39916 |
| -131.8547 | 0.5699 | 0.74247 | 29.5433 | 0.70741 | 0.48935 |
| -127.2042 | 0.52653 | 0.84396 | 34.1938 | 0.7282 | 0.57361 |
| -122.5536 | 0.47708 | 0.94073 | 38.8443 | 0.71679 | 0.65523 |
| -117.9031 | 0.42138 | 1.0302 | 43.4948 | 0.68527 | 0.72935 |
| -113.2526 | 0.35981 | 1.11 | 48.1453 | 0.64907 | 0.82382 |
| -108.6021 | 0.29319 | 1.1779 | 52.7958 | 0.60545 | 0.91627 |
| -103.9516 | 0.22265 | 1.2321 | 57.4464 | 0.55314 | 1.004 |
| -99.301 | 0.14963 | 1.2712 | 62.0969 | 0.49191 | 1.0844 |
| -94.6505 | 0.075185 | 1.294 | 66.7474 | 0.4223 | 1.1552 |
| -90 | 0 | 1.3 | 71.3979 | 0.34547 | 1.214 |
| -85.3495 | -0.058986 | 1.2925 | 76.0484 | 0.26305 | 1.2592 |
| -80.699 | -0.11723 | 1.2681 | 80.699 | 0.17707 | 1.2893 |
| -76.0484 | -0.17406 | 1.2275 | 85.3495 | 0.095485 | 1.3031 |
| -71.3979 | -0.22839 | 1.1717 | 90 | 0.01933 | 1.3 |
| -66.7474 | -0.27882 | 1.1022 | 94.6505 | -0.06876 | 1.294 |
| -62.0969 | -0.32418 | 1.0209 | 99.301 | -0.14963 | 1.2712 |
| -57.4464 | -0.36369 | 0.92987 | 103.9516 | -0.22265 | 1.2321 |
| -52.7958 | -0.39694 | 0.83154 | 108.6021 | -0.29319 | 1.1779 |
| -48.1453 | -0.42412 | 0.7285 | 113.2526 | -0.35981 | 1.11 |
| -43.4948 | -0.4461 | 0.62344 | 117.9031 | -0.42138 | 1.0302 |

| | | | | | |
|-----------|------------|----------|----------|----------|----------|
| -38.8443 | -0.4648 | 0.52359 | 122.5536 | -0.47708 | 0.94073 |
| -34.1938 | -0.48374 | 0.41948 | 127.2042 | -0.52653 | 0.84396 |
| -29.5433 | -0.49509 | 0.32843 | 131.8547 | -0.5699 | 0.74247 |
| -24.8927 | -0.4992 | 0.25045 | 136.5052 | -0.60809 | 0.63897 |
| -23.8191 | -0.50837 | 0.2343 | 141.1557 | -0.64299 | 0.53621 |
| -22.7455 | -0.50902 | 0.21885 | 145.8062 | -0.67813 | 0.43693 |
| -21.6719 | -0.52126 | 0.2041 | 150.4567 | -0.69521 | 0.34377 |
| -20.5982 | -0.53079 | 0.19004 | 155.1073 | -0.69515 | 0.25921 |
| -19.5246 | -0.53762 | 0.17668 | 156.8853 | -0.67832 | 0.22964 |
| -18.451 | -0.54176 | 0.16402 | 158.6634 | -0.64415 | 0.20176 |
| -17.3774 | -0.54322 | 0.15205 | 160.4414 | -0.59047 | 0.1757 |
| -16.3037 | -0.54203 | 0.14078 | 162.2195 | -0.53679 | 0.15155 |
| -15.2301 | -0.53819 | 0.1302 | 163.9975 | -0.48311 | 0.12941 |
| -14.1565 | -0.53172 | 0.12032 | 165.7756 | -0.42943 | 0.10936 |
| -13.0829 | -0.51544 | 0.11114 | 167.5536 | -0.37575 | 0.091484 |
| -12.0092 | -0.4899 | 0.10265 | 169.3317 | -0.32207 | 0.075847 |
| -9.862 | -0.47217 | 0.087768 | 171.1097 | -0.26839 | 0.062511 |
| -7.9793 | -0.43034 | 0.079284 | 172.8878 | -0.21472 | 0.051529 |
| -5.9841 | -0.35129 | 0.071596 | 174.6658 | -0.16104 | 0.042943 |
| -3.9647 | -0.2449 | 0.065036 | 176.4439 | -0.10736 | 0.036785 |
| -2.0015 | -0.12582 | 0.059697 | 178.2219 | -0.05368 | 0.033082 |
| -0.009897 | 0.00088021 | 0.055187 | 180 | 0 | 0.031845 |

SD7032- Above Rated

| α (deg) | C_l | C_d | α (deg) | C_l | C_d |
|----------------|----------|----------|----------------|----------|----------|
| -180 | 0 | 0.031845 | 0.999709 | 0.037038 | 0.032234 |
| -178.222 | 0.053679 | 0.033082 | 1.981167 | 0.1372 | 0.032283 |
| -176.444 | 0.107358 | 0.036785 | 2.991704 | 0.259146 | 0.032365 |
| -174.666 | 0.161036 | 0.042943 | 3.973598 | 0.387711 | 0.032473 |
| -172.888 | 0.214715 | 0.051529 | 4.981807 | 0.521556 | 0.032611 |
| -171.11 | 0.268394 | 0.062511 | 5.990598 | 0.648728 | 0.032776 |
| -169.332 | 0.322073 | 0.075847 | 6.972463 | 0.757747 | 0.03296 |
| -167.554 | 0.375751 | 0.091484 | 7.982622 | 0.84619 | 0.033171 |
| -165.776 | 0.42943 | 0.109361 | 8.964895 | 0.900909 | 0.033397 |
| -163.998 | 0.483109 | 0.12941 | 9.977121 | 0.937821 | 0.036011 |
| -162.219 | 0.536788 | 0.151552 | 10.96123 | 0.969127 | 0.042807 |
| -160.441 | 0.590466 | 0.175701 | 11.97302 | 0.991846 | 0.05371 |
| -158.663 | 0.644145 | 0.201763 | 12.95637 | 1.000149 | 0.067673 |
| -156.885 | 0.678315 | 0.229636 | 13.97139 | 0.926977 | 0.085105 |
| -155.107 | 0.695149 | 0.259214 | 14.98213 | 0.790872 | 0.10505 |
| -150.457 | 0.695209 | 0.343772 | 15.96446 | 0.714804 | 0.126465 |
| -145.806 | 0.678126 | 0.436928 | 17.95721 | 0.699072 | 0.174277 |
| -141.156 | 0.642987 | 0.536207 | 19.95119 | 0.693742 | 0.225011 |

University of Maine's Advanced Structures and Composites Center

Report Number: 23-57-1183

| | | | | | |
|----------|----------|----------|----------|----------|----------|
| -136.505 | 0.608087 | 0.638966 | 24.89273 | 0.823866 | 0.340211 |
| -131.855 | 0.569905 | 0.742471 | 29.54325 | 0.822503 | 0.428789 |
| -127.204 | 0.52653 | 0.843963 | 34.19377 | 0.830838 | 0.516526 |
| -122.554 | 0.477076 | 0.940734 | 38.84429 | 0.810868 | 0.604543 |
| -117.903 | 0.421377 | 1.030199 | 43.49481 | 0.7708 | 0.687243 |
| -113.253 | 0.359812 | 1.10996 | 48.14533 | 0.726044 | 0.78592 |
| -108.602 | 0.293188 | 1.177874 | 52.79585 | 0.67387 | 0.882584 |
| -103.952 | 0.222654 | 1.232109 | 57.44637 | 0.613011 | 0.974528 |
| -99.301 | 0.149627 | 1.271189 | 62.09689 | 0.54323 | 1.059165 |
| -94.6505 | 0.075185 | 1.294036 | 66.74741 | 0.465069 | 1.134098 |
| -90 | 0 | 1.3 | 71.39792 | 0.379682 | 1.197185 |
| -85.3495 | -0.04937 | 1.291296 | 76.04844 | 0.288709 | 1.246592 |
| -80.699 | -0.098 | 1.26571 | 80.69896 | 0.194174 | 1.280844 |
| -76.0484 | -0.14522 | 1.22389 | 85.34948 | 0.104037 | 1.298864 |
| -71.3979 | -0.18994 | 1.166916 | 90 | 0.01933 | 1.3 |
| -66.7474 | -0.23075 | 1.096262 | 94.65052 | -0.06876 | 1.294036 |
| -62.0969 | -0.26651 | 1.013762 | 99.30104 | -0.14963 | 1.271189 |
| -57.4464 | -0.2964 | 0.921557 | 103.9516 | -0.22265 | 1.232109 |
| -52.7958 | -0.32004 | 0.822047 | 108.6021 | -0.29319 | 1.177874 |
| -48.1453 | -0.3376 | 0.717815 | 113.2526 | -0.35981 | 1.10996 |
| -43.4948 | -0.34997 | 0.61157 | 117.9031 | -0.42138 | 1.030199 |
| -38.8443 | -0.35906 | 0.510532 | 122.5536 | -0.47708 | 0.940734 |
| -34.1938 | -0.36839 | 0.405232 | 127.2042 | -0.52653 | 0.843963 |
| -29.5433 | -0.37012 | 0.312998 | 131.8547 | -0.56991 | 0.742471 |
| -24.8927 | -0.36462 | 0.23383 | 136.5052 | -0.60809 | 0.638966 |
| -23.8191 | -0.37157 | 0.217409 | 141.1557 | -0.64299 | 0.536207 |
| -22.7455 | -0.37 | 0.201685 | 145.8062 | -0.67813 | 0.436928 |
| -21.6719 | -0.39068 | 0.186657 | 150.4567 | -0.69521 | 0.343772 |
| -20.5982 | -0.40864 | 0.172326 | 155.1073 | -0.69515 | 0.259214 |
| -19.5246 | -0.4239 | 0.158691 | 156.8853 | -0.67832 | 0.229636 |
| -18.451 | -0.43647 | 0.145752 | 158.6634 | -0.64415 | 0.201763 |
| -17.3774 | -0.44637 | 0.13351 | 160.4414 | -0.59047 | 0.175701 |
| -16.3037 | -0.45361 | 0.121964 | 162.2195 | -0.53679 | 0.151552 |
| -15.2301 | -0.4582 | 0.111115 | 163.9975 | -0.48311 | 0.12941 |
| -14.1565 | -0.46017 | 0.100961 | 165.7756 | -0.42943 | 0.109361 |
| -13.0829 | -0.45232 | 0.091504 | 167.5536 | -0.37575 | 0.091484 |
| -12.0092 | -0.43521 | 0.082744 | 169.3317 | -0.32207 | 0.075847 |
| -9.862 | -0.43435 | 0.067312 | 171.1097 | -0.26839 | 0.062511 |
| -7.9793 | -0.41273 | 0.057633 | 172.8878 | -0.21472 | 0.051529 |
| -5.98414 | -0.35188 | 0.04796 | 174.6658 | -0.16104 | 0.042943 |
| -3.96475 | -0.26098 | 0.039764 | 176.4439 | -0.10736 | 0.036785 |
| -2.00146 | -0.15456 | 0.03429 | 178.2219 | -0.05368 | 0.033082 |
| -0.0099 | -0.03869 | 0.032217 | 180 | 0 | 0.031845 |

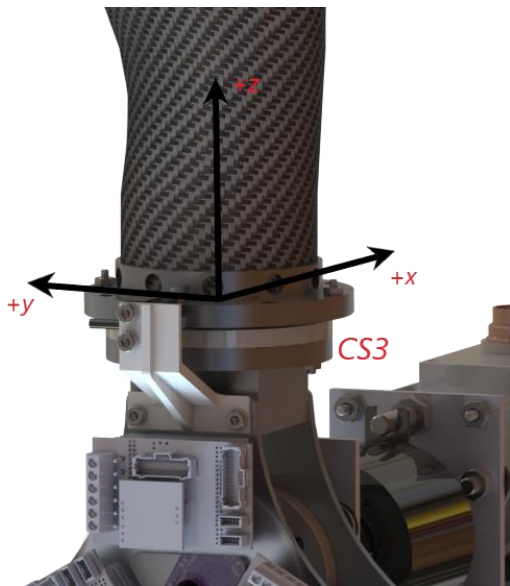
Cylinder

| α (deg) | C_l | C_d |
|----------------|----------|----------|
| -1.80E+02 | 0.00E+00 | 1.00E+00 |
| 0.00E+00 | 0.00E+00 | 1.00E+00 |
| 1.80E+02 | 0.00E+00 | 1.00E+00 |

Undistributed Individual Blade Structural Properties (Model Scale)

| Blade | Mass (kg) | CMz (m) | Ixx (kg*m ²) | Iyy (kg*m ²) |
|----------------------------|-----------|---------|--------------------------|--------------------------|
| 1 | 0.23658 | 0.537 | 0.1161 | 0.1210 |
| 3 | 0.23466 | 0.540 | 0.1161 | 0.1203 |
| 4 | 0.23553 | 0.540 | 0.1160 | 0.1242 |
| Spare (7) | 0.23683 | 0.533 | 0.1160 | 0.1196 |
| Average of blade in-use | 0.23559 | 0.539 | 0.1161 | 0.1218 |

Note: Z-axis is along the blade from root to tip. Bending about Y-axis is flapwise bending, as shown below



Appendix C: OpenFAST Model

The as-built OpenFAST model developed alongside this campaign is available at
https://github.com/UMaine-W2/FOCAL_OpenFast_C4